

Contents

| | |
|---|------------|
| Neutrino Mass and Mixing | 119 |
| 1 Introduction | 119 |
| 2 Basic Properties of Neutrinos | 120 |
| 3 Neutrino Counting | 123 |
| 4 Cosmology and Astrophysics | 124 |
| 5 Supernova Constraints on Neutrino Masses | 124 |
| 6 Direct Mass Measurements | 126 |
| 7 Double Beta Decay | 129 |
| 8 Neutrino Oscillations | 130 |
| 9 Masses Below 10^{-2} eV (Solar Neutrinos) | 131 |
| 10 Atmospheric Neutrinos | 136 |
| 11 Reactor Neutrinos | 140 |
| 12 Accelerator Neutrinos | 142 |
| 13 Summary | 147 |
| References | 148 |

NEUTRINO MASS AND MIXING

PAUL LANGACKER

University of Pennsylvania, Philadelphia, PA 19104

REGINA RAMEIKA

Fermi National Accelerator Laboratory, Batavia, IL 60510

HAMISH ROBERTSON

University of Washington, Seattle, WA 98195

Neutrino Mass Working Group Members

| | | | |
|---------------|---|--------------|--|
| D. Ayres | <i>Argonne National Laboratory</i> | B. Bernstein | <i>Fermi National Accelerator Laboratory</i> |
| B. Blumenfeld | <i>John Hopkins University</i> | A. Capone | <i>Universita La Sapienza/INFN</i> |
| M. Diwan | <i>Brookhaven National Laboratory</i> | G. Domokos | <i>Johns Hopkins University</i> |
| F. Federspiel | <i>Los Alamos National Laboratory</i> | T. Gaisser | <i>Bartol Research Institute</i> |
| M. Goodman | <i>Argonne National Laboratory</i> | K. Heller | <i>University of Minnesota</i> |
| A. Hime | <i>Los Alamos National Laboratory</i> | T. Kycia | <i>Brookhaven National Laboratory</i> |
| K. Lande | <i>University of Pennsylvania</i> | M. Lowry | <i>Princeton University</i> |
| A. Mann | <i>University of Pennsylvania</i> | M. Murtagh | <i>Brookhaven National Laboratory</i> |
| P. Rosen | <i>University of Texas at Arlington</i> | N. Stanton | <i>Kansas State University</i> |
| R. Steinberg | <i>Drexel University</i> | R. Stokstad | <i>Lawrence Berkeley Laboratory</i> |
| B. Vogelaar | <i>Princeton University</i> | H. White | <i>Los Alamos National Laboratory</i> |

1 Introduction

There are strong theoretical and experimental motivations to search for neutrino mass. The Standard Model of electroweak interactions provides the framework in which the fundamental particles are arranged into pairs and generations (or flavors) of quarks:

$$\begin{pmatrix} u \\ d \end{pmatrix} \quad \begin{pmatrix} c \\ s \end{pmatrix} \quad \begin{pmatrix} t \\ b \end{pmatrix}$$

and of leptons:

$$\begin{pmatrix} e^- \\ \nu_e \end{pmatrix} \quad \begin{pmatrix} \mu^- \\ \nu_\mu \end{pmatrix} \quad \begin{pmatrix} \tau^- \\ \nu_\tau \end{pmatrix}$$

Experimentally, the neutrinos appear to be massless, and hence the assumption that they are exactly so is built into the basic Standard Model. However, despite the experimental success of the model, we know that it is incomplete. In particular, many of the major outstanding challenges in particle physics today have to do with the question of mass. For example, we ask, “Why is the top

quark so heavy?” (or “Why are the other fermions so light?”), “Is the Higgs particle the origin of mass?”, and “Are the neutrinos really massless?” There are also a number of persisting questions in cosmology and astrophysics, such as “Where are the solar neutrinos?”, “Are there missing atmospheric neutrinos?” and “What makes up the mass of the universe?”.

In the minimal Standard Model and in certain extensions such as SU(5), neutrinos are assumed massless. The Standard Model can, however, easily accommodate massive neutrinos without contradicting firmly established symmetries, so the existence of neutrino mass is an open experimental question. Direct measurements of neutrino masses have yielded only upper limits (≤ 5.1 eV, ≤ 0.27 MeV, and ≤ 31 MeV for electron, muon, and tau neutrinos, respectively [1]). Non-zero neutrino masses below these limits contradict neither theory nor experiment. The exciting possibility is that massive, flavor-mixed neutrinos (*e.g.*, $\nu_e \rightarrow \nu_\mu$) may answer many of the above questions. The next generation of oscillation and direct mass measurements will extend sensitivities into ranges of mass and mixing parameters for which a positive

result is likely. This could well constitute the first break with the standard model. Alternatively, the experiments should be able to exclude cleanly most of the interesting parameter range. In either case, the implications for particle physics, astrophysics, and cosmology will be significant.

Almost all extensions of the standard model predict non-zero neutrino masses. Both general directions for new physics – grand unification/superstrings and compositeness – are likely to lead to neutrino masses. Many models predict seesaw-type masses, $m_\nu \sim m_D^2/M$, where m_D is a typical quark or charged lepton mass and M is the scale of new physics. Such theories naturally explain why the neutrino masses are so small. Measuring these masses and the leptonic mixings would probe the physics at the underlying mass scale M and would be an excellent complement to searches at high-energy colliders. Large values for M (e.g., 10^{12} GeV, as expected in many grand unified theories), predict masses relevant to the solar neutrinos (e.g., $\nu_e \rightarrow \nu_\mu$) and to hot dark matter (e.g., ν_τ).

Observation of non-zero neutrino masses could well shed light not only on new physics, but also on the origin of fermion masses in general, which are among the least understood aspects of the standard model.

During the last decade, several scientific developments have given us reasons to believe that neutrinos may indeed be massive. Recent results by COBE and other groups on angular variations of the temperature of the cosmic background radiation [2] as well as the observed clustering of galaxies on very large scales may be explained by a significant component of hot dark matter [3]. The most economical hypothesis for providing such hot dark matter is to assume that τ neutrinos, which are a component of the primordial radiation field, have a mass somewhere in the range from 5 to 35 eV. The precise mass value depends on the Hubble constant and on the fraction of the cosmic energy density contributed by hot dark matter, but a typical estimate is $m_{\nu_\tau} \sim 7$ eV. If true, neutrinos could well be among the dominant constituents of the universe! As we shall see later in this report, most of this interesting parameter range can be probed in planned short baseline oscillation experiments, supplemented with direct mass searches and neutrinoless double beta decay experiments. The latter is also sensitive to the nature of the neutrino mass. Observation of a nearby supernova would extend the sensitivity to very small or zero mixing.

A second and perhaps more direct experimental indication that neutrinos have mass comes from the detection of solar neutrinos. All solar neutrino experiments observe a deficit of neutrinos compared to the expectations of standard solar models. The gallium results are now significantly below the predictions of almost all solar models. Even more compelling, the relative suppressions

observed in the Homestake and Kamiokande experiments imply a distortion of the ^8B spectrum, which is inconsistent with any conventional astrophysical explanation, and strongly suggestive of non-standard neutrino properties. Neutrino oscillation effects are expected to be exaggerated by passage through solar matter. This “MSW effect” provides the simplest and most natural explanation, adequately describing all data for Δm^2 around 10^{-5} eV². Planned and proposed solar neutrino experiments have the potential for cleanly confirming or refuting MSW and other hypotheses, independent of solar model uncertainties. They should also allow a model-independent determination of the major neutrino flux components, even in the presence of oscillations, and therefore serve as a powerful tool for solar astronomy.

Three experiments indicate a deficit in the ratio of muon and electron neutrinos produced in cosmic ray interactions. This ratio is relatively free of theoretical ambiguities in the incident fluxes, and hints at neutrino oscillations with $\Delta m^2 \sim 1 - 10^{-3}$ eV² and large mixing angles. These possibilities could be definitely established or excluded by proposed long baseline experiments.

LEP results on the Z lineshape indicate that there are only three light active (left-handed) neutrinos, and limits from big bang nucleosynthesis severely constrain the parameter space allowed for sterile neutrinos. These results, combined with the experimental and theoretical clues described above, significantly limit the possibilities and the likely parameter space for neutrino mass and oscillations. The program of experiments that are planned or proposed for the next decade could unambiguously establish neutrino masses or exclude almost all of the likely possibilities.

A serious program to probe neutrino masses and mixings in the ranges suggested by hot dark matter, atmospheric neutrinos, and solar neutrinos, as well as many well-motivated theoretical ideas (such as grand unification through supersymmetry), has a real possibility of observing positive signals. These could well be the first break with the standard model of particle physics, could have profound consequences for cosmology, and would serve as a quantitative probe of the solar core. Even negative results would severely constrain the possibilities for new physics beyond the standard model, would exclude one of the major possibilities for the dark matter, and would be a powerful tool for studying the sun.

2 Basic Properties of Neutrinos

There are literally hundreds of models of neutrino mass [4]. The nomenclature, notation, and variety of models are very confusing. In this section, we give an overview of the basic concepts and principal classes of models.

The first concept is that of a Weyl neutrino. A Weyl fermion is the basic two-component fermionic degree of

freedom. A left-handed state ν_L is necessarily related by a CP or CPT transformation to a right-handed antiparticle state by

$$\nu_L \xleftrightarrow[CP]{} \nu_R^c \equiv C\bar{\nu}_L^T, \quad (1)$$

where C is the charge conjugation matrix, given by $C = i\gamma^2\gamma^0$ in the Bjorken-Drell conventions.^a Thus the L and R states are essentially adjoints of each other. It is a matter of convenience which is defined as the particle and which is the antiparticle. Sometimes it is useful to define all right-handed states as antiparticles; when there is a conserved lepton number it is convenient to label the leptons as particles and the antileptons as antiparticles.

An important distinction is between active (SU_2 -doublet) and sterile^b (SU_2 -singlet) neutrinos. The former have normal weak interactions, while the latter have no weak interactions except those induced by mixing. In the standard model with an additional sterile Weyl neutrino N_R , one has

$$\begin{pmatrix} \nu_e \\ e^- \end{pmatrix}_L \xleftrightarrow[CP]{} \begin{pmatrix} e^+ \\ \nu_e^c \end{pmatrix}_R \quad N_R \xleftrightarrow[CP]{} N_L^c. \quad (2)$$

The ν_e and its partner are active, associated in weak doublets with the electron, while the extra N_R is sterile with no weak interactions. In the ordinary standard model one introduces three active massless neutrinos ν_{eL} , $\nu_{\mu L}$, $\nu_{\tau L}$ and no sterile states.

Mass terms induce transitions between right and left-handed states. A Dirac mass term, which conserves lepton number, involves transitions between two different Weyl neutrinos, ν_L and N_R (or ν_R^c and N_L^c). That is, the right-handed state N_R is different from ν_R^c . The form is

$$-\mathcal{L}_{\text{Dirac}} = m_D(\bar{\nu}_L N_R + \bar{N}_R \nu_L) = m_D \bar{\nu} \nu, \quad (3)$$

where the Dirac field is defined as $\nu \equiv \nu_L + N_R$. Thus a Dirac neutrino has four components ν_L , ν_R^c , N_R , N_L^c , and the mass term allows a conserved lepton number $L = L_\nu + L_N$. This and other types of mass terms can easily be generalized to three or more families, in which case the masses become matrices. In that case, the charged current transitions involve a leptonic mixing matrix (analogous to the Cabibbo-Kobayashi-Maskawa (CKM) quark mixing matrix), which can lead to neutrino oscillations between the light neutrinos.

For an ordinary Dirac neutrino the ν_L is active and the N_R is sterile. The transition between these states is $\Delta I = \frac{1}{2}$, where I is the weak isospin. The mass requires

^aThe subscripts L and R really refer to the left and right chiral projections. In the limit of zero mass these correspond to left and right helicity states.

^bSterile neutrinos are often referred to as ‘‘right-handed’’ neutrinos, but that terminology is confusing and inappropriate when Majorana masses are present.

SU_2 breaking and is generated by a Yukawa coupling

$$-\mathcal{L}_{\text{Yukawa}} = h_\nu(\bar{\nu}_e \bar{e})_L \begin{pmatrix} \varphi^0 \\ \varphi^- \end{pmatrix} N_R + H.C. \quad (4)$$

One has $m_D = h_\nu v/\sqrt{2}$, where the vacuum expectation value (VEV) of the Higgs doublet is $v = \sqrt{2}\langle\varphi^0\rangle = (\sqrt{2}G_F)^{-1/2} = 246$ GeV, and h_ν is the Yukawa coupling. A Dirac neutrino mass is just like a quark or charged lepton mass, but that leads to the question of why neutrino mass is so small. One would require $h_{\nu_e} < 10^{-10}$ in order to have $m_{\nu_e} < 10$ eV. For this reason most people do not take normal Dirac masses seriously. However, some caution is advised since we do not understand the patterns of quark or charged lepton masses either. One interesting idea is to invoke some sort of symmetry that requires $h_\nu = 0$ at tree-level, so that neutrino masses would only be generated at the loop level and might naturally be small. However, there are no compelling or simple models to implement this otherwise attractive idea. Something of this sort may be one possibility for superstring models, in which it is difficult to implement the simplest version of the seesaw mechanism. (Non-renormalizable operators are another possibility.)

A variant form of Dirac neutrino is the Zeldovich, Konopinski, Mahmoud (ZKM) type [5], for which ν_L and N_R are both active states – the N_R is just a right-handed antineutrino associated with a different family than the ν_L . For example, one could have $N_{eR} = \nu_{\tau R}^c$ as the partner of the ν_{eL} . In this case $L_e - L_\tau$ would be conserved and ν_{eL} , ν_{eR}^c , $\nu_{\tau R}^c$, $\nu_{\tau L}$ would be the four components of the ZKM neutrino. Similarly, one could choose $N_{eR} = \nu_{\mu R}^c$, so that $L_e - L_\mu$ would be conserved. The ZKM case is defined as a Dirac neutrino by most authors, because it has a (somewhat unusual) conserved lepton number and has four components. However, a ZKM neutrino requires a more complicated Higgs structure than doublets, and in many ways is more analogous to the Majorana neutrinos to be described below. In fact a ZKM neutrino is a limiting case of Majorana neutrinos, and not all authors agree that it should be referred to as a Dirac neutrino.

A Majorana mass, which violates lepton number by two units ($\Delta L = \pm 2$), makes use of the right-handed antineutrino, $N_R = \nu_R^c$, rather than a separate Weyl neutrino. It is a transition from an antineutrino into a neutrino. Equivalently, it can be viewed as the creation or annihilation of two neutrinos, and if present it can therefore lead to neutrinoless double beta decay. The form of a Majorana mass term is given in Eq. 5.

$$\begin{aligned} -\mathcal{L}_{\text{Majorana}} &= \frac{1}{2}m(\bar{\nu}_L \nu_R^c + \bar{\nu}_R^c \nu_L) + \\ &= \frac{1}{2}m(\bar{\nu}_L C \bar{\nu}_L^T + H.C.) + \end{aligned}$$

$$= \frac{1}{2} m \bar{\nu} \nu \quad (5)$$

$\nu = \nu_L + \nu_R^c$ is a self-conjugate two-component state satisfying $\nu = \nu^c = C \bar{\nu}^T$. If ν_L is active then the above transition involves $\Delta I = 1$ and m must be generated by either an elementary Higgs triplet or by an effective operator involving two Higgs doublets arranged to transform as a triplet.

For an elementary triplet $m \sim h_T v_T$, where h_T is a Yukawa coupling and v_T is the triplet VEV. The simplest implementation is the Gelmini-Roncadelli (GR) model [6], in which lepton number is spontaneously broken by v_T . The original GR model is now excluded by the LEP data on the Z width. The decay $Z \rightarrow M \chi$, in which M is the Majoron (the Goldstone boson associated with the spontaneous breaking of lepton number) and $\chi \simeq \text{Re } \varphi_T^0$ is a physical scalar field with mass $m_\chi = O(v_T)$, occurs rapidly and contributes $\Delta N'_\nu = 2$ to the effective number of neutrino flavors. Since, $N'_\nu = 2.988 \pm 0.023$ [7] there is no room for this decay. Variant models involving explicit lepton number violation or in which the Majoron is mainly a weak singlet (*invisible* Majoron models) are still possible.

If the mass, m , is generated by an effective operator, one expects $m \sim C v^2/M$, where C is a dimensionless constant and M is the scale of the new physics which generates this operator. The most familiar example is the seesaw model, to be discussed below.

All of the effects of lepton number violation associated with Majorana masses are proportional to the mass, and there is no distinction between Dirac and Majorana neutrinos in the limit $m \rightarrow 0$ unless there are new interactions. For $m \rightarrow 0$ both reduce to a Weyl neutrino with the standard model interactions, and the N_R decouples in the Dirac case.

It is also possible to consider mixed models in which both Majorana and Dirac mass terms are present. For two Weyl neutrinos one has a mass term

$$-L = \frac{1}{2} (\bar{\nu}_L \bar{N}_L^c) \begin{pmatrix} m_T & m_D \\ m_D & m_S \end{pmatrix} \begin{pmatrix} \nu_R^c \\ N_R \end{pmatrix} + H.C., \quad (6)$$

where $\nu_L \leftrightarrow \nu_R^c$ and $N_L^c \leftrightarrow N_R$ are the two Weyl states. m_T and m_S are Majorana masses which transform as weak triplets and singlets, respectively (assuming that the states are respectively active and sterile), while m_D is a Dirac mass term. Diagonalizing this 2×2 matrix one finds that the physical particle content is given by two Majorana mass eigenstates $n_i = n_{iL} + n_{iR}^c$, $i = 1, 2$; as usual these are two-component objects ($n_i = n_i^c$) constructed from the Weyl neutrinos $n_{iL} \leftrightarrow n_{iR}^c$.

There are a number of important special cases of the general mixed model:

- The simplest is that of pure Majorana masses, $m_D = 0$, in which the two Majorana eigenstates are just

the original active and sterile neutrinos: $n_{1L} = \nu_L$, $n_{2L} = N_L^c$.

- Another important case is the Dirac limit, $m_T = m_S = 0$. When one diagonalizes the mass matrix in the Dirac limit the two Majorana mass eigenstates

$$\begin{aligned} n_1^D &= \frac{1}{\sqrt{2}}(\nu_L + N_L^c) + \frac{1}{\sqrt{2}}(\nu_R^c + N_R) \\ n_2^D &= \frac{1}{\sqrt{2}}(\nu_L - N_L^c) - \frac{1}{\sqrt{2}}(\nu_R^c - N_R) \end{aligned} \quad (7)$$

are degenerate with mass m_D , and can be combined to form a Dirac neutrino with a conserved lepton number. Thus, a Dirac neutrino can be viewed as a pair of degenerate Majorana neutrinos with 45° mixing and opposite CP parity.

- The pseudo-Dirac case $m_T \ll m_D$, $m_S \ll m_D$ is a perturbation on the Dirac limit. The Majorana mass terms lead to a small splitting of the mass eigenstates, *i.e.*, one has two almost-degenerate Majorana neutrinos and a small breaking of L . For example, consider the case $m_S = 0$, $m_T \ll m_D$. One obtains two Majorana neutrinos

$$n_1 = n_1^D + \frac{m_T}{4m_D} n_2^D, \quad n_2 = -\frac{m_T}{4m_D} n_1^D + n_2^D, \quad (8)$$

with masses

$$m_{1,2} = m_D \pm m_T/2. \quad (9)$$

Thus, one can have $\nu_L \rightarrow N_L^c$ oscillations with near maximal mixing.

- In the seesaw limit [8], $m_T = 0$, $m_D \ll m_S$, one obtains two Majorana neutrinos

$$\begin{aligned} n_{1L} &\simeq \nu_L - \frac{m_D}{m_S} N_L^c \\ n_{2L} &\simeq \frac{m_D}{m_S} \nu_L + N_L^c \end{aligned} \quad (10)$$

with masses

$$\begin{aligned} m_1 &\sim \frac{m_D^2}{m_S} \ll m_D \\ m_2 &\sim m_S. \end{aligned} \quad (11)$$

Thus, there is one heavy neutrino and one neutrino much lighter than the typical Dirac scale. Such models are a popular and natural way of generating neutrino masses much smaller than the other fermion masses.

There are literally hundreds of versions of the seesaw and related models [4]. The heavy scale m_S can range anywhere from the TeV scale to the Planck scale. The TeV scale models are motivated, for example, by left-right symmetric models [9]. Typically,

the Dirac masses m_D are of the order of magnitude of the corresponding charged lepton masses, so that one expects masses of order 10^{-1} eV, 10 keV, and 1 MeV for the ν_e , ν_μ , and ν_τ , respectively. (The latter two violate cosmological bounds unless they decay rapidly and invisibly.) Intermediate scales, such as $10^{12} - 10^{16}$ GeV, are motivated by grand unification and typically yield masses in the range relevant to hot dark matter, and solar and atmospheric neutrino oscillations. The grand unified theories often imply Dirac masses $m_D \sim m_u$, where m_u is the mass of the up-type quark of the corresponding family. Depending on whether there is also a family hierarchy of heavy masses m_S , the light masses

$$m_{\nu_i} \sim C_i \frac{m_{u_i}^2}{m_{S_i}}, \quad (12)$$

of the i^{th} family may vary approximately quadratically with m_{u_i} (the quadratic seesaw) or linearly (the linear seesaw) [10]. $C_i \sim (0.05 - 0.4)$ in (12) is a radiative correction. Typical light neutrino masses in the quadratic seesaw are (10^{-7} eV, 10^{-3} eV, 10 eV) for $M_{S_i} \sim 10^{12}$ GeV (the intermediate seesaw, expected in some superstring models or in grand unified theories with multiple breaking stages). Such masses would cause $\nu_e \rightarrow \nu_\mu$ oscillations in the sun, and make ν_τ be a dark matter candidate (or, for a somewhat smaller ν_τ mass, $\nu_\mu \rightarrow \nu_\tau$ atmospheric neutrino oscillations). Similarly, for $M_{S_i} \sim 10^{16}$ GeV (the grand unified seesaw, expected in old-fashioned grand unified theories with large Higgs representations) one typically finds smaller masses around (10^{-11} eV, 10^{-7} , 10^{-2} eV), suggesting $\nu_e \rightarrow \nu_\tau$ oscillations in the sun. In such models one often (but not always) finds that the lepton and quark mixing matrices are similar.

One can easily generalize the mixed models in Eq. (6) to three or more fermion families. For three families there will be three active and three sterile neutrinos. These will mix to form six Majorana mass eigenstates and a 6×6 mixing matrix. One would in general expect both oscillations of the active neutrinos into each other (known as first class or flavor oscillations) and also (second class) oscillations of the active neutrinos into sterile neutrinos. However, the latter are only significant if the Dirac and Majorana mass terms are of comparable magnitude (*i.e.*, the mass eigenstates that are predominantly active and sterile have comparable masses). This does not occur naturally in most models (it does not occur at all for pure Dirac or Majorana masses, and is strongly suppressed in the seesaw models), so that oscillations between active and sterile neutrinos, while a logical possibility, are perhaps less likely than flavor oscillations.

A very different class of models are those in which

the neutrino masses are zero at the tree level (typically because no Weyl singlets or elementary Higgs triplets are introduced), but only generated by loops [11], *i.e.*, radiative generation. Such models are very attractive in principle and explain the smallness of m_ν . However, the actual implementation generally requires the *ad hoc* introduction of new Higgs particles with nonstandard electroweak quantum numbers and lepton number-violating couplings. There are a great variety of these models. When phenomenological constraints are imposed they often have a pseudo-Dirac neutrino, *e.g.*, in which $L_e - L_\mu + L_\tau$ is approximately conserved. Many of the models were motivated by attempts to generate a large value for the neutrino magnetic moment μ_ν [12] (suggested by hints of possible time dependence in the Homestake solar neutrino rate) without generating a large value of the effective neutrino mass $\langle m_{\nu_e} \rangle$ relevant to neutrinoless double beta decay.

3 Neutrino Counting

- There are $N_\nu \geq 2$ Weyl neutrinos in Nature, because the ν_e and ν_μ have been directly observed.
- We also know that $N_\nu \geq 3$, because the interactions of the τ are not suppressed by mixing. There must therefore be a separate ν_τ . (SU_2 gauge invariance requires that each doublet involves a different neutrino state.)
- One has $N'_\nu \equiv , Z \rightarrow \text{inv}/, Z \rightarrow \nu\bar{\nu} = 2.988 \pm 0.023$ from the LEP measurements of the invisible Z width $, Z \rightarrow \text{inv} = , Z - , Z \rightarrow \text{vis}$ [7]. N'_ν counts the active neutrinos with masses $m \ll M_Z/2$, and also includes contributions from heavy active neutrinos up to the kinematic limit with an additional phase space suppression. It does not count sterile neutrinos. Other light invisible states also contribute. For example, a triplet Majoron [6] yields $\Delta N'_\nu = 2$, which is clearly excluded, while a doublet Majoron [13] or a light scalar neutrino in supersymmetry each contribute $\Delta N'_\nu = \frac{1}{2}$.
- There is a limit $N''_\nu < 3.3$ at 95% CL from the observed abundance of helium and other light elements [14]. This bound is complementary to the LEP limit. It includes neutrinos only for masses up to $m < O(30 \text{ MeV})$. However, in addition to active neutrinos it includes sterile neutrinos ν_S for a wide range of masses and mixing with active states [15], for which the sterile neutrinos would have been produced in the early universe prior to nucleosynthesis. In particular, for oscillations into sterile neutrinos the parameter range relevant to laboratory experiments and atmospheric neutrinos is excluded, as can be seen in Figure 1. Nucleosynthesis allows $\nu_e \rightarrow \nu_S$ for solar neutrinos via the MSW effect on the small

angle (nonadiabatic) but not the large angle branch^c

4 Cosmology and Astrophysics

There are many constraints from cosmology and astrophysics on neutrino masses, life-times, and other properties [17]. One of the most important is the limit

$$\sum m_i < 35 \text{ eV}, \quad (13)$$

where the sum extends over the light, stable, active neutrinos. (Also included are sterile neutrinos with a significant mixing with the ordinary neutrinos [15]). If (13) does not hold, then there would be too much energy density in the present universe. If neutrinos are unstable there are a large variety of other constraints [17]. If the neutrinos decay via normal weak interactions then the decays would be either $\nu_2 \rightarrow \nu_1 \gamma$ or $\nu_1 e^+ e^-$, depending on the masses. There are many limits on such decays from the present energy density, the properties of the microwave background radiation, supernovae and nucleosynthesis. The result is that for such unstable neutrinos one must still have $m_{\nu_\mu, \nu_\tau} < 35 \text{ eV}$.

The limit in (13) can be evaded if the neutrinos decay or annihilate into invisible decay products. In this case, one has the weaker limit [17],

$$m_\nu < 35 \left[\frac{T_0}{\tau_\nu} \right]^{\frac{1}{2}} \text{ eV}, \quad (14)$$

where T_0 is the age of the present universe and τ_ν is the neutrino lifetime, to ensure that their decay products will have redshifted to a low enough energy. Other constraints follow from the fact that structure can only grow in a matter-dominated universe [18]. In principle, one could have decays of a heavier neutrino into three lighter neutrinos, but it is difficult to find models in which the decay is sufficiently rapid. More promising are decays $\nu_2 \rightarrow \nu_1 G$ or $\bar{\nu}_1 G$, where G is a Goldstone boson, such as a Majoron^d(for a spontaneously broken lepton number) or a familon (for a broken family symmetry). There are many laboratory and astrophysical restrictions on such models [4,17].

5 Supernova Constraints on Neutrino Masses

The detection of neutrinos^e from SN 1987A in the Kamiokande II (KII) [19] and Irvine-Michigan-Brookhaven (IMB) [20] detectors on February 23, 1987

^cIn fact, the present solar neutrino data are most likely inconsistent with a large angle solution for sterile neutrinos.

^dOne can also have the annihilation of two neutrinos into two Majorons.

^eThis section is based on materials prepared by Andrew Hime, LANL.

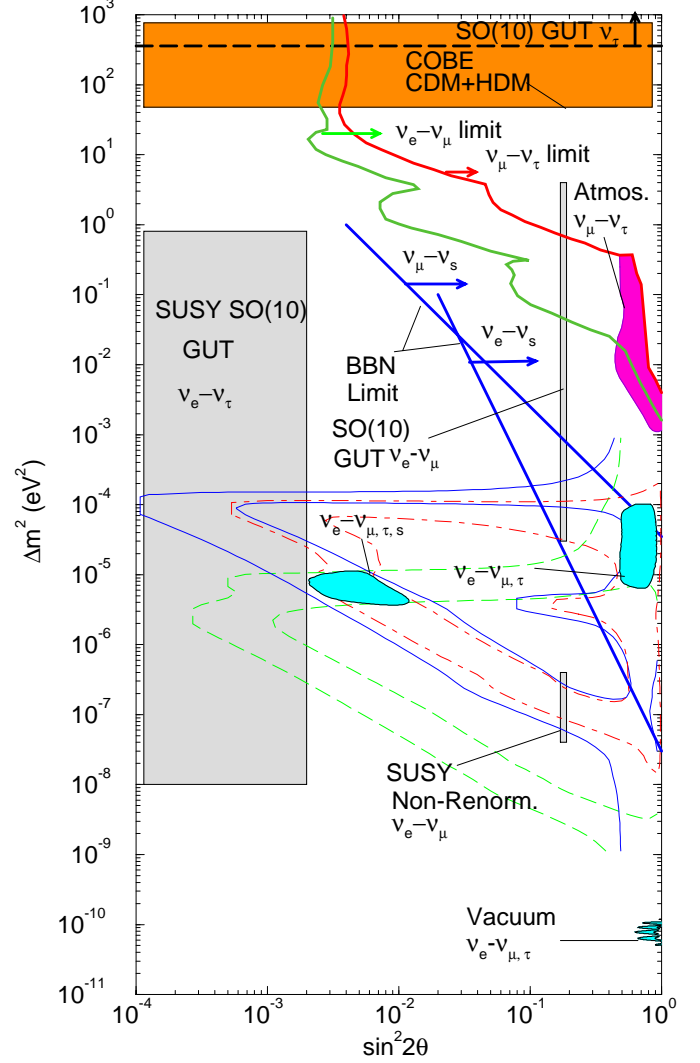


Figure 1: Allowed and excluded regions in the neutrino oscillation parameters $\Delta m^2 - \sin^2\theta$. Shown are the regions excluded by laboratory experiments (upper right), and by big bang nucleosynthesis for oscillations into sterile neutrinos (to right of solid lines). Also indicated are the regions suggested by solar neutrinos (MSW or vacuum oscillations), atmospheric neutrinos, and a hot dark matter component of the universe, as well as predictions of some specific seesaw models. From [16].

confirmed the characteristic duration, energetics, and overall gross structure including the antielectron neutrino content of the burst [21]. A total of some 19 events attributable to the supernova were recorded, and hundreds of interpretations of the data in terms of upper and lower limits on neutrino mass were offered. The variety of conclusions speaks to the considerable model-dependence of the supernova burst structure as well as uncertainties related to experimental sensitivity, timing, and background. In a thoughtful retrospective, Lamb and Loredo [22] concluded that an upper limit of about 25 eV at the 95% confidence level could be set on the mass of ν_e from the supernova data. Neutral current signatures from muon and tau neutrinos were absent since the IMB and KII detectors were not sufficiently sensitive.

A neutrino with a mass of a few eV would contribute significantly to the closure density of the universe. Precision measurements of the tritium endpoint rule out the electron neutrino as the dominant dark matter in the universe, unless significant amounts of both hot and cold dark matter exist [3], as does the limit on neutrinoless double beta decay for Majorana ν_e . Muon and tau neutrino masses in the cosmologically interesting regime are unlikely to be determined directly in any foreseeable terrestrial experiment. Consequently, the detection of neutrino bursts from supernovae may present our best hope for directly inferring a neutrino mass of cosmological significance. (Short baseline laboratory oscillation experiments will probe this range if there is non-negligible $\nu_\mu - \nu_\tau$ mixing.)

5.1 Neutrinos from Supernovae

In *The Future of Supernova Detection*, Burrows, Klein, and Ghandi [23] describe generic models of supernovae in our own galaxy, and discuss the response for a number of representative Čerenkov detectors and scintillation neutrino telescopes to a nearby neutrino burst. The supernova model employed by Burrows *et al.* assembles a number of modern calculations. While not representative of a specific event it is meant to be realistic in terms of gross structure, temperature, energy, and time scale. Figure 2 displays the initial electron neutrino spike due to the release of trapped neutronization neutrinos as the initial shock breaks out of the core. The ringing that follows is not necessarily a feature that will occur in most supernovae. There then follows a longer period of thermal decay during which the neutrino flux drops according to a power law until the neutron star becomes transparent to neutrinos, at which time (~ 50 seconds) neutrino emission ceases. Burrows *et al.* point out that limits on the electron neutrino mass as low as 1 eV could be set if the initial breakout were observed; otherwise, uncertainties in supernova modeling make it difficult to derive limits competitive with direct terrestrial experiments.

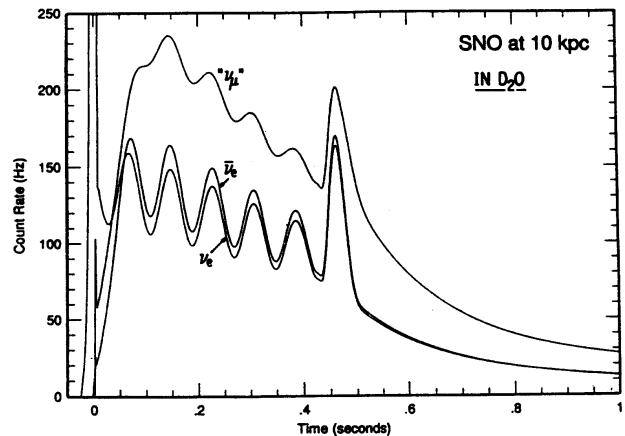


Figure 2: Interaction rates for all neutrino flavors in the SNO detector using a generic supernova model at 10 kpc. The designation “ ν_μ ” denotes the total contributions from both muon and tau neutrinos and their antiparticles. From Burrows *et al.* [23].

5.2 Supernova Neutrinos in SNO

The unique capability of the Sudbury Neutrino Observatory (SNO) [24] (see also Section 9.3.1) to measure the neutral-current interaction of all active neutrino species makes it possible to determine a muon or tau neutrino mass in the cosmologically significant range by studying the lengthening in flight time of a massive neutrino species from a distant supernova. The effect of a 20 eV and 50 eV tau neutrino mass is shown in Figure 3a for a generic supernova at 10 kpc (the center of our galaxy). Even if only one neutrino species has a significant mass, all species and their antiparticles will contribute to the total neutral-current rate in SNO. The effect of a single massive species is shown in Figure 3b, and can be recovered with sufficient statistics by comparison to the charged-current data from electron and antielectron neutrinos. The comparison is complicated by the very different temperatures of the neutrino sources of different flavors [25].

Given a galactic supernova, about 270 neutral-current and 150 charged-current events are expected to be registered in the heavy water component of SNO as well as 350 charged-current events in the outer light water shield. Approximately one third of these events would arrive during the first half-second, during which the delayed arrival of 20 eV neutrinos would be most evident. Assuming about 30% neutron detection efficiency, a neutrino mass in the 20 - 50 eV range would constitute a ~ 3 standard-deviation effect. If neutral current events are converted to Čerenkov light by radiative neutron capture, then the charged and neutral-current spectra need

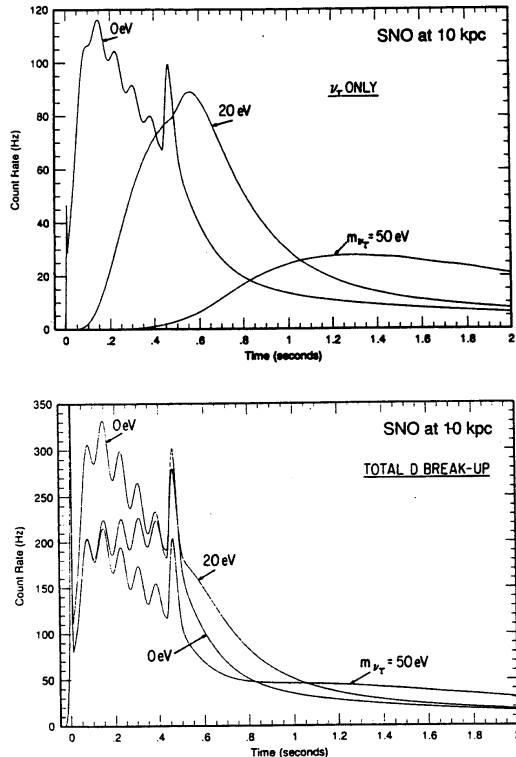


Figure 3: Neutral-current rates in the SNO detector for the generic supernova model of Burrows *et al.* [23]. In (a) the spectrum is shown for the case of a single massive neutrino species. In (b) the total deuteron disintegration rate is shown for the case of a single massive neutrino and two massless species.

to be decomposed via the light water charged-current signal. It is therefore planned to deploy ^3He proportional counters in the SNO detector [25] to obtain a continuous and distinct measure of the neutral-current signal.

5.3 An International Network of Detectors

The upgrade of KII to SuperKamiokande (SK) and construction of the Large Volume Detector (LVD) [26] will allow very high statistics measurements of the ν_e and $\bar{\nu}_e$ signal during the first second of a supernova burst. The characteristic rise-time of 50 msec in SK and LVD for a massless neutrino is lengthened to 300 msec for a 10 eV electron neutrino [23]. This method of neutrino mass determination cannot be applied to the muon and tau neutrinos without implementing a neutral-current based detector such as SNO or the proposed Supernova Burst Observatory (SNBO) [27]. It is desirable to combine the unique features of a variety of future neutrino detectors to optimize our ability to extract physics from a supernova burst. For example, muon and/or tau neutrino

masses could be determined by employing the combined signals from different detectors. The large mass and high sensitivity to electron antineutrinos in SK [28] would provide the time of stellar collapse, while the subsequent time shift associated with the onset of the ν_μ and/or ν_τ signal in a neutral-current based detector could be employed to constrain or determine the ν_μ and/or ν_τ mass [29].

A number of unique detectors, either under construction or proposed, have been discussed in references [23] and [29], both with respect to their ability in elucidating our understanding of stellar collapse and to the prospects for detection of a cosmologically significant neutrino mass. The next generation of underground neutrino detectors can serve to determine a neutrino mass in the 15 to 100 eV range. Depending upon one's confidence in the predictive power of supernova burst models the lower end of this range might be pushed down to 5 eV [29]. Pennypacker *et al.* estimate a galactic core-collapse supernova at least every 31 ± 7 years [30]. Hence, over the next decade the probability of such an occurrence is $\sim 20\text{-}30\%$, a sufficiently high probability that every effort must be made to capitalize upon the physics associated with such an event.

6 Direct Mass Measurements

The most obvious way to explore the question of neutrino mass is to consider the kinematics of the weak decays of the e , μ , and τ leptons. In this section we will review the experimental efforts to measure the masses of ν_e , ν_μ , and ν_τ using kinematics.

6.1 Direct Measurement of m_{ν_e}

A neutrino with mass around 7 eV is a leading candidate [3] for the hot dark matter component of the universe suggested by the COBE and galaxy distribution results [2]. Barring a new supernova, direct (kinematic) determinations of the masses of the neutrinos are within striking distance of this mass only in the case of ν_e .

For ν_e , the current generation of tritium beta decay experiments set upper limits on the $\bar{\nu}_e$ mass at about this level. Thus improved experiments, down to the 1 or 2 eV level, as well as admixture searches in this mass range, must be a significant priority in future efforts. At the same time note must be taken of a curious feature of the current experiments: the central value of neutrino mass-squared is negative in all cases. The average of 5 experiments yields $m_{\nu_e}^2 = -96 \pm 21 \text{ eV}^2$, almost a $5\text{-}\sigma$ effect. (The parametrization in terms of $m_{\nu_e}^2$ is only a convenient way to describe a "bump" that appears near the endpoint of the tritium spectrum.) Such a statistically unlikely result suggests the presence of some as yet unidentified systematic error common to the experiments, such as an

unexpectedly large problem in the calculation of the excitation spectrum of the residual molecular ion THe^+ , or the presence of new particle physics. Speculations on new physics include tachyonic neutrinos, capture from a (very dense) relic cosmic sea of neutrinos which would produce a monoenergetic peak at or above the endpoint, and admixture of a massive neutrino with strong final-state interactions that would produce a bump at or below the endpoint. Such possibilities are exciting, even if unlikely, and demand that improved experiments be performed to verify or reject them.

Another approach [31] is a study of the beta spectrum of ^{187}Re (endpoint of 2.64 keV *vs* ^3H of 18.6 keV) using the developing cryogenic calorimetric technique. It offers the exciting capability of eliminating two of the major sources of systematic uncertainty, energy loss in the source, and atomic final state distributions. There are, however, significant technical challenges that must be overcome before a successful measurement can be carried out.

New experimental work on the tritium spectrum is nearing completion in Russia [32] with an intense molecular tritium source and a very high-resolution retarding-field analyzer.

A summary of the existing experimental limits on the direct m_{ν_e} is given in Table 1.

There is an anomaly seen at the endpoint of the tritium spectrum in three experiments on pure T_2 that far exceeds statistical fluctuations. The current published experimental results (*post* 1988) are consistent with each other, but not with $m_{\nu_e} = 0$ and standard Fermi β decay. In this circumstance, it is difficult to assign a confidence level to an upper limit on the mass. Qualitatively, a mass greater than 10 eV can confidently be ruled out, but the situation is clearly unsatisfactory.

A plan of action might include the following ingredients:

- Continuing current laboratory work on the tritium decay. Experiments are still in progress at Troitsk [32], Mainz [37], Austin [40], and Yorktown Heights [39].
- Evaluation of the possibility of reactivating the Los Alamos and Livermore experiments.
- Experiments to measure atomic-physics parameters of the decay of T_2 to THe^+ , such as the branch to (at least) the ground state, radiative decays from excited states, 1- and 2-electron shakeoff probabilities, infrared spectra, and resonances in H-He collisions as a check on the crucially important final-state spectrum calculations.
- New measurements of the $\text{T}-^3\text{He}$ mass difference.
- An atomic T experiment, where the final-state spectrum becomes trivial. Spin-polarized tritium at low temperatures might form the basis for a compact, intense atomic source.

- Bolometric (calorimetric) measurements on tritium or ^{187}Re .
- Continued theoretical examination of exotic possibilities, such as a gross error in the theory of the two-electron molecule, high densities of relic neutrinos, and non-standard electroweak models.

6.2 Direct Measurement of m_{ν_μ}

The most precise data on the mass of ν_μ come from measurements of the μ momentum following the decay of stopped pions. The most recent determination of the mass of the π^+ by Jeckelmann *et al.* [41], coupled with the muon data of Abela *et al.* [42], give

$$m_{\nu_\mu}^2 \leq -0.097(72) \text{ MeV}^2, \quad (15)$$

which, with the Bayesian procedure described by the Particle Data Group [1], yields an upper limit of 270 keV at 90% confidence on the mass of ν_μ . A result slightly more than $1-\sigma$ negative is not unexpected if the true value is zero.

However, a new round of experiments at the Paul Scherrer Institute has now reached such a high level of precision that a serious problem in this approach has been discovered. Table 2 gives the recent history of these measurements.

As indicated, with the mass of the charged pion published by Jeckelmann *et al.*, the central value for m_ν^2 is over 5σ negative. The reason for this is now, it appears, understood. The mass of the π^+ has been deduced from pionic X-ray spectra. The X-ray lines have a fine structure corresponding to the presence of zero, one, or two K-shell vacancies. The data on the $4f - 3d$ line in ^{24}Mg show only two components of significant intensity, allowing for two possible assignments of structure. Auger widths, which depend sensitively on the K-vacancy probability, were used to resolve the ambiguity in favor of the ‘‘B’’ solution, but both new results on pionic X-ray intensity ratios and new calculations of the strong absorption widths now favor the opposite choice [46], *i.e.*, the ‘‘A’’ solution. With the ‘‘A’’ solution, the central value for m_{ν_μ} is (by chance) exactly 0, and an upper limit of 270 keV on m_{ν_μ} at 90% CL can be derived.

Stopped π decay is approaching a limit where theoretical uncertainty (in deducing the masses of the π^+ and the μ^+) is limiting the accuracy with which m_ν can be determined. One novel approach was that of Anderhub *et al.* [47], who used a magnetic ‘racetrack’ and π decay in flight to obtain,

$$m_{\nu_\mu}^2 = -0.14(20) \text{ MeV}^2 \quad (16)$$

$$m_{\nu_\mu} \leq 500 \text{ keV (90\%CL)} \quad (17)$$

The method is (by design) relatively insensitive to m_π and m_μ , and could potentially offer an avenue for further

Table 1: Existing limits on the square of the electron neutrino mass.

| Institute/Location | Year | Source State | Mass ² , eV ² ± stat. ± syst. | Limit, eV (95%CL) | Ref. |
|--------------------|-------|----------------------|--|--------------------------------|------|
| ITEP, Moscow | 88 | Valine-T | +676 ± 235 | = 26 ₅ ⁶ | [33] |
| Los Alamos | 91 | T ₂ gas | -147 ± 68 ± 41 | ≤ 9.3 | [34] |
| Univ. of Zürich | 91 | OTS-T | -24 ± 48 ± 61 | ≤ 11 | [35] |
| INS, Tokyo | 91 | Cd Arach.-T | -65 ± 85 ± 65 | ≤ 13 | [36] |
| Mainz Univ. | 93 | T ₂ solid | -39 ± 34 ± 15 | ≤ 7.2 | [37] |
| LLNL (Chem.) | 94 | T ₂ gas | -130 ± 20 ± 15 | - | [38] |
| INR, Moscow | Run'g | T ₂ gas | | | [32] |
| IBM, Yktn Hts | Stdby | Metal-T | | | [39] |
| UTx/Brandeis | R&D | T ₂ gas | | | [40] |

Table 2: Limits on mu neutrino mass from $\pi^+ \rightarrow \mu^+ + \nu_\mu$ at rest.

| Collaboration | Ref. | m_μ , MeV | p_μ , MeV/c | m_π , MeV | m_ν^2 , MeV ² |
|-----------------------------|------|----------------|-----------------|---------------|------------------------------|
| Abela <i>et al.</i> 84 | [42] | 105.65932(29) | 29.79139(83) | 139.56761(77) | -0.163(80) |
| Jeckelmann <i>et al.</i> 86 | [41] | | | 139.56871(53) | -0.097(72) |
| PDG 92 ^a | [43] | 105.658387(34) | | 139.56737(33) | |
| Daum <i>et al.</i> 91 | [44] | | 29.79206(68) | 139.56996(67) | |
| Frosch <i>et al.</i> 92 | [45] | | 29.79144(20) | | -0.127(25) |
| Jeckelmann <i>et al.</i> 94 | [46] | “A” solution: | | 139.56995(35) | 0.000(45) |
| | | “B” solution: | | 139.56782(37) | -0.127(46) |

^a Electron mass down 8 ppm

improvement. No direct measurement scheme is known that can access the cosmologically interesting mass range below 100 eV, other than time-of-flight from a supernova.

6.3 Direct Measurement of m_{ν_τ}

Of the three neutrinos now known to exist, the tau neutrino is arguably the least well understood. Not only has it never been directly observed, but the limits on its mass are orders of magnitude less stringent than those on its electron and muon neutrino cousins [1].

Studies placing the most stringent limits on the tau neutrino mass, m_{ν_τ} , have used the spectrum of the invariant mass of the measured tau decay products, M_X . The maximum attainable M_X in a given tau decay mode is a function of m_{ν_τ} . This measurement is most sensitive to events with $M_X \sim M_\tau$ since this is where the spectrum varies most dramatically as a function of m_{ν_τ} . The tau decay final states with the least energy available for the tau neutrino are generally more sensitive to m_{ν_τ} and recent studies have concentrated on high-multiplicity tau decays largely for this reason. Previous limits on m_{ν_τ} are given in Table 3.

In the next few years, any improvement in the limit

on m_{ν_τ} at e^+e^- colliders will come from improved statistics using techniques that rely on obtaining an event near the kinematic limit $M_X = M_\tau$. While experiments at LEP and CESR can all do these analyses, the poorer mass resolution on M_X and smaller (though purer) sample sizes at the LEP experiments places them at a competitive disadvantage relative to CLEO-II.

CLEO-II will continue to accumulate large amounts of data, and will probably update the analyses of the $\tau \rightarrow 5\pi\nu_\tau$ and $\tau \rightarrow 3\pi 2\pi^0\nu_\tau$ decays in an attempt to set an improved limit on m_{ν_τ} . As with earlier analyses of these decay modes, luck plays a regrettably large role in the stringency of the limit one can set, since the probability of getting an event very close to the kinematic limit is exceedingly small. The tau decay to the final state $3\pi\pi^0\nu_\tau$, while peaked lower in invariant mass than the five pion decay modes, has a much larger branching fraction and therefore may have a similar sensitivity to m_{ν_τ} .

Decay modes with kaons are potentially more sensitive to m_{ν_τ} by virtue of the reduced q^2 available to the ν_τ . Although the CLEO-II detector has relatively poor $K-\pi$ separation, sufficient statistics make using the fi-

Table 3: Existing limits on the tau neutrino mass.

| Expt. | Year | Final State | Events | Limit (95% CL, MeV) | Ref. |
|---------|------|-------------------------------------|--------|------------------------|------|
| DELCO | 85 | $KK\pi\nu_\tau, K\pi\pi\nu_\tau$ | 4 | 157 | [48] |
| MARK-II | 85 | $5\pi\pi^0\nu_\tau$ | 3 | 125 | [49] |
| MARK-II | 85 | $3\pi(\pi^0)\nu_\tau$ | 22 | 143 | [50] |
| ARGUS | 85 | $3\pi\nu_\tau$ | 1536 | 70 | [51] |
| HRS | 86 | $5\pi(\pi^0)\nu_\tau$ | 13 | 76 | [52] |
| CLEO | 87 | $3\pi(\pi^0)\nu_\tau$ | 9135 | 85 | [53] |
| ARGUS | 88 | $5\pi\nu_\tau$ | 12 | 31 | [54] |
| CLEO-II | 93 | M_τ | – | 75 | [55] |
| CLEO-II | 93 | $5\pi\nu_\tau, 3\pi 2\pi^0\nu_\tau$ | 113 | 33 | [56] |

nal states $K\pi\pi\nu_\tau$ and $KK\pi\nu_\tau$ feasible. The final state $K_s K_s \pi\nu_\tau$ may also be usable. Decay modes with kaons may be *less* sensitive, however, if their spectral functions cause the 3-prong invariant mass spectrum to be peaked at lower masses than that of the 5-pion decays.

With the advent of very high statistics (10^7 - 10^8 τ pairs) event samples at either B or τ - c (Tau-Charm) factories, the technique described above will be superseded by one which relies on statistical subtraction of backgrounds. Improved detector resolutions and particle identification techniques will also play important roles.

Monte Carlo studies assuming 10^8 τ pairs predict a sensitivity to a τ neutrino with a mass as low as 2 MeV at a τ - c Factory, and as low as 2.5 MeV at a B Factory [57]. These estimates are the combined result of $5\pi\nu_\tau$, $3\pi 2\pi^0\nu_\tau$, and $KK\pi\nu_\tau$ decay mode analyses, and assume resolutions of 2-5 MeV on the invariant masses of the final state particles.

7 Double Beta Decay

Double beta decay^f is a very rare process, with a half-life of order 10^{20} years, in which a metastable nucleus (A, Z) transforms into its next nearest neighbor ($A, Z+2$) and emits two electrons [4]. In the standard electroweak model, two antineutrinos always accompany the electrons and share the 1 – 3 MeV energy released on a roughly equal basis. In theories going beyond the standard model, it becomes possible for the two electrons to be emitted either by themselves alone, or accompanied by a light scalar particle, the Majoron. These two double beta decay modes violate lepton number conservation, and their existence would imply that at least one neutrino is a Majorana particle with non-zero mass.

The half-life for the two-neutrino decay mode can be

^fThis section is based on material prepared by Peter Rosen, Univ. Texas at Arlington.

calculated directly from the standard model, and can be written

$$\frac{1}{T_{2\nu}} = G_{2\nu} |M_{2\nu}|^2, \quad (18)$$

where $G_{2\nu}$ is a phase space integral and $M_{2\nu}$ is the nuclear matrix element. Much theoretical progress has been made in recent years in our understanding of the two-neutrino matrix elements, which tend to be small. Since the no-neutrino decay mode vanishes in the absence of neutrino mass, its half-life depends directly upon an “effective” mass $\langle m_{\nu_e} \rangle$,

$$\frac{1}{T_{0\nu}} = G_{0\nu} |M_{0\nu}|^2 \left[\frac{\langle m_{\nu_e} \rangle}{m_e} \right]^2, \quad (19)$$

where

$$\langle m_{\nu_e} \rangle = \sum_i m_i \lambda_i U_{ei}^2 \quad (20)$$

involves a sum over all light ($\ll 30$ MeV) Majorana neutrino mass eigenstates, m_i , weighted by the CP parities ($\lambda_i = \pm 1$) and the squares U_{ei}^2 of the mixing matrix elements^g. For heavier m_i there is an additional propagator suppression in the contribution to $\langle m_{\nu_e} \rangle$.

An important diagnostic tool in distinguishing between different decay modes is the spectrum of energy carried by the two electrons. For two-neutrino decay, the spectrum is continuous with a broad peak just below the mid-point and a very flat approach to zero at the end-point; in fact, it vanishes for all practical purposes in the last 20% of the range. For no-neutrino decay, the spectrum is a spike at the end-point because the two electrons carry all the available energy. The spectrum for the Majoron mode is continuous, but peaks towards the end-point, in the region where the two-neutrino spectrum

^g $\langle m_{\nu_e} \rangle$ vanishes for Dirac neutrinos, which can be interpreted as two degenerate Majorana neutrinos ($m_1 = m_2 = m_D$) with $U_{e1} = U_{e2} = \frac{1}{\sqrt{2}}$ and opposite CP eigenphases.

vanishes. Thus any events occurring in the last 20% of the spectrum must either be background, or signals for non-standard double beta decay modes.

Double beta decay has been the object of experimental searches for more than forty years. The earliest experiments invoked the “geochemical method” in which one probes ancient ores rich in the parent nucleus (for example, ^{82}Se or ^{130}Te) searching for traces of the noble gas daughter nuclei (^{82}Kr or ^{130}Xe). This method allows one to establish the existence of the double beta decay transition and measure its lifetime, but does not determine which mode, or modes are actually occurring. In the most recent experiment of this kind [58], the half-life of ^{128}Te was measured to be $(7.7 \pm 0.4) \times 10^{24}$ years.

Searches specifically aimed at detecting the no-neutrino mode have been performed with germanium crystals, which serve as both source (^{76}Ge , 8% natural abundance) and detector, and which measure the total energy of the emitted electrons. The most recent experiments use 90% enriched crystals [59] and give a lower limit on the half-life of 3×10^{24} years, which corresponds to an upper bound on $\langle m_{\nu_e} \rangle$ of about 1 eV. This is the best limit available to date. Actual observation of the decay would imply that at least one of the Majorana mass eigenstates must be heavier than

$$m_i^{\max} > 1 \text{ eV} \left[\frac{10^{24} \text{ yrs}}{T_{0\nu}({}^{76}\text{Ge})} \right]^{1/2}. \quad (21)$$

The first direct observation of two-neutrino double beta decay in the laboratory was made in 1986 with a xenon-filled time-projection chamber [60]. Electron tracks were observed directly and timing was used to exclude background events. Spectra consistent with two-neutrino decay were observed in ^{82}Se , ^{100}Mo , and ^{150}Nd , and the corresponding half-lives measured. In the case of ^{82}Se , the result was consistent with the geochemical measurement. More elaborate versions of this technique are being developed.

Future experiments will concentrate on the search for the no-neutrino mode because of its implications for physics beyond the standard model. As the bounds on the effective mass $\langle m_{\nu_e} \rangle$ go down, so the experiments will have to grow bigger and more ambitious, as in the case of the NEMO collaboration in France, or they will have to develop new cryogenic techniques, as is happening in the area of solar neutrinos.

8 Neutrino Oscillations

A direct consequence of neutrino mass is that the flavor eigenstates,^h ν_e , ν_μ , ν_τ , are actually a linear combina-

^h As described in Section 2, it is also possible in principle to have oscillations between active and sterile neutrinos. However, these are less likely theoretically, and most of the interesting pa-

tions of massive neutrinos, ν_1 , ν_2 and ν_3 . For simplicity, we use a two component formulation such that

$$\begin{aligned} \nu_e &= \nu_1 \cos \theta + \nu_2 \sin \theta \\ \nu_\mu &= -\nu_1 \sin \theta + \nu_2 \cos \theta \end{aligned}$$

This is analogous to the well understood phenomena of mass mixing in the quark sector. Because neutrinos are only weakly interacting and ultra relativistic, the mass eigenstates, ν_1 and ν_2 will evolve in time. Therefore, one can derive a probability that a neutrino that starts out as flavor a can be found at a later time as flavor b . This probability is typically expressed in terms of the mixing angle, θ , the mass-squared difference $\Delta m^2 = m_2^2 - m_1^2$ (in eV^2) between the two mass states, and an experimental ratio L/E :

$$P(\nu_a \rightarrow \nu_b) = \sin^2 2\theta \sin^2 (1.27 \Delta m^2 L/E), \quad (22)$$

where L is the distance (in km) from the original source of the neutrinos to where the probability is being measured, and E is the energy of the neutrinos in GeV. This concept of oscillation is familiar to the particle physicist from the oscillation phenomena observed in the neutral kaon system.

For a given θ and Δm^2 the oscillation probability varies periodically with time or distance. One does not know *a priori* the values of θ and Δm^2 , and, because the probability depends on the ratio L/E , there are many regimes of particle physics in which oscillation searches can take place.

There are two types of experiment to search for neutrino oscillations. Most, including the solar and reactor measurements, are called “disappearance” experiments. This means that a source of neutrinos of a single flavor is created and the flux is measured at two different places separated by a distance. Differences in the flux at the two locations will indicate that neutrinos have oscillated into a different flavor. Alternatively, in an “appearance” experiment a source of neutrinos of a single flavor will travel a distance to a target where they can interact. Observation of a lepton of flavor different from the original beam will indicate that neutrinos have oscillated. Results of experimental searches for neutrino oscillations are displayed on plots in $\sin^2 2\theta$ vs Δm^2 parameter space, as in Figure 1. The oscillation channels most easily explored are $\nu_\mu \leftrightarrow \nu_e$, $\nu_\mu \rightarrow \nu_\tau$, $\bar{\nu}_e \rightarrow X$, and $\nu_\mu \rightarrow X$, where X is any neutrino type, including one which does not interact (sterile). In the following four sections we will review the status of experimental searches for neutrino oscillations. We begin with the long-standing solar-neutrino puzzle and progress being made toward confirming or denying neutrino oscillations as an explanation of the puzzle. We will then address the more recently discovered anomaly in the atmospheric neutrino experiments. Finally we will

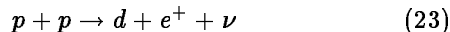
parameter range (except for solar neutrinos) is excluded by primordial nucleosynthesis.

discuss the status of oscillation searches that can be performed with neutrino beams produced at nuclear reactors and particle accelerators.

9 Masses Below 10^{-2} eV (Solar Neutrinos)

Solar neutrinos provide, at present, the only available way to reach masses in the range 10^{-2} to 10^{-5} eV. Neutrino oscillations which occur in vacuum [61] or which may be amplified by passage through solar material (the MSW effect [62,63]), can deplete the flux of ν_e by converting some of them into ν_μ , ν_τ , or a sterile species. The observations made with the four experiments performed so far indicate a flux at the earth that is consistently below the results of astrophysical calculations. Moreover, the relative rates in the different types of experiment indicate that the largest depletion is in the middle of the spectrum (the ${}^7\text{Be}$ line and the low energy part of the ${}^8\text{B}$ spectrum), which is inconsistent with any known astrophysical or nuclear explanation [64,65,66,67,68,69,70]. On the other hand, the data from all four experiments can be described well in terms of calculations which include the MSW-enhanced neutrino-oscillation effect. The deficit of electron-type neutrinos thus provides suggestive evidence for a nonzero neutrino mass and nonconservation of lepton family number.

The solar neutrino spectrum is dominated by the first step in nuclear burning, the pp reaction,



with a continuous neutrino spectrum ending at 420 keV. From there, several competing pathways lead to ${}^4\text{He}$. In addition, a catalytic process involving carbon, nitrogen and oxygen isotopes (CNO) accounts for a few percent of hydrogen burning. The fluxes and energies of neutrinos from the sun in the standard Bahcall-Pinsonneault [71] model are given in Table 4.

Experimentally, the higher energy neutrinos from ${}^8\text{B}$ decay are the easiest to detect, but they originate in a reaction branch that plays a negligible role in energy production in the sun.

9.1 Experiments Now in Operation

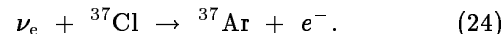
The low energies of solar neutrinos have severely taxed the ingenuity of experimentalists. Cross sections are small and the events compete with ubiquitous backgrounds. Two general types of experiment have been devised to overcome these difficulties, the radiochemical method and ‘active’ (*i.e.*, electronic) detection. Detectors must be large, and they must be deep underground.

We review briefly the four currently-operating experiments and then describe the experiments that are being developed and which will begin to operate in about two

years. Finally, we summarize some of the possibilities among proposed future experiments.

9.1.1 The Chlorine Experiment

In this, the first solar neutrino experiment [72], neutrinos are detected in a target of 615 tons of perchloroethylene (C_2Cl_4) 1500 meters underground in the Homestake Gold Mine in Lead, South Dakota. The target isotope, ${}^{37}\text{Cl}$, can capture a neutrino, producing a radioactive isotope ${}^{37}\text{Ar}$:



The reaction can occur for electron neutrinos with energy greater than 0.814 MeV. The neutrino reactions are registered by extracting and counting the decays of ${}^{37}\text{Ar}$ ($\tau = 35$ days) in a proportional counter. The present result from runs 18 through 120 over the years 1970-93 is 2.55(23) SNU, whereas the expected rate [71] is 8.0(10). (1 SNU = 10^{-36} interactions per target atom per second.) Over the 25 years this experiment has been in operation, many refinements and tests have been made. The most significant was the introduction in 1970 of the rise-time of the ionization pulse as a means of distinguishing the point-like decays of ${}^{37}\text{Ar}$ from the longer tracks produced by background events – it was this strategy that disclosed a true solar neutrino signal above background. More recently, events have been analyzed according to probability distributions rather than cuts in energy-rise-time space, the muon-induced background has been remeasured [the current best estimate [72] is 0.047(16) atoms per day, somewhat lower than the value in general use, 0.08(3)], counter efficiencies have been redetermined with attention to losses in handling the argon (leading to a 3% increase in the flux) [73], and the cross section for detection of ${}^8\text{B}$ neutrinos has been re-evaluated [74].

Because the Cl-Ar experiment (and its relationship to Kamiokande) plays an important role in conclusions about the likelihood of neutrino oscillations, a popular pastime has been to search for internal inconsistencies in the experiment, particularly in the form of apparent time dependence or nonstatistical behavior. By selecting certain groups of data points, it is possible to find disagreements with the average, but little evidence for nonstatistical behavior has been demonstrated. The experiment is also frequently characterized as ‘uncalibrated’, and it is true that a test with an artificial neutrino source has not been done. However, extensive calibrations in which, for example, ${}^{37}\text{Ar}$ has been produced *in situ* by neutron reactions and measured, show that the experiment behaves as expected.

Table 4: Solar neutrino fluxes at the earth calculated by Bahcall and Pinsonneault.

| Source | Flux, $10^{10} \text{ cm}^{-2}\text{s}^{-1}$ | 1σ , % | E_{max} , MeV |
|-----------------|--|---------------|--|
| pp | 6.0 | 0.7 | 0.420 |
| pep | 0.014 | 1.7 | 1.442 (line) |
| ^7Be | 0.49 | 5 | 0.862 (line, 90%) 0.384 (line, 10%) |
| ^8B | 0.00057 | 12 | 15 |
| ^{13}N | 0.049 | 17 | 1.199 |
| ^{15}O | 0.043 | 19 | 1.732 |
| ^{17}F | 0.00054 | 15 | 1.740 |

9.1.2 The Kamiokande Experiment

Kamiokande (Kamioka Nucleon Decay Experiment) is a 3,000-ton water Cerenkov detector with a fiducial volume of 680 tons for solar neutrinos [75,76]. The reaction observed is the elastic scattering of neutrinos by electrons,

$$\nu + e^- \rightarrow \nu + e^- . \quad (25)$$

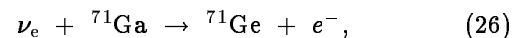
At the energies of interest for solar neutrino detection, reaction (25) is about six times more likely for ν_e than for ν_μ or ν_τ . Despite a significant background from radioactivity of the rocks in the mine, from radioactivity in the water, and from cosmic-ray induced events, neutrino interactions can be detected at the rate of about one per week above a threshold of 7.5 MeV because the electrons struck by neutrinos recoil preferentially in the direction from the sun to the earth. Kamiokande, the first “active” (electronic rather than radiochemical) solar-neutrino experiment, has shown three very important things: first, the detected neutrinos do indeed come from the sun, second, the observed flux is about half that predicted by the standard solar model; and, third, that the spectrum is consistent with the expected ^8B β spectrum. The current result [77] is $0.51 \pm 0.04 \pm 0.06$ of the Bahcall-Pinsonneault [71] flux, $5.69 \times 10^6 \text{ cm}^{-2}\text{s}^{-1}$.

9.1.3 The Gallium Experiments

The pp neutrinos are too low in energy to be detected by either the chlorine-argon or the Kamiokande experiment. Since pp neutrinos are the most abundant, their flux is more reliably predicted than any other [78], being determined mainly by the solar luminosity and only weakly dependent on details of the sun’s interior. Consequently, the measurement of the flux of pp neutrinos has long been seen [79,80] as potentially a decisive method for searching for neutrino disappearance.

Two radiochemical experiments that can detect pp neutrinos are currently in operation; they use ^71Ga as

their target via the process



which has an energy threshold of 0.233 MeV. As in the chlorine experiment, radioactive atoms of ^71Ge are extracted and counted. The standard-model prediction is that after a month of operation about 16 atoms of ^71Ge will be present in 30 tons of gallium.

One of the gallium experiments, SAGE [81,82] (the Soviet-American Gallium Experiment) is operating in the Baksan Laboratory in the Russian Caucasus Mountains. SAGE currently uses 60 tons of gallium metal. The other experiment, Gallex [83,84], is a European-American-Israeli collaboration operating in the Gran Sasso tunnel near Rome, Italy. Gallex uses 30 tons of gallium in a $\text{GaCl}_3\text{-HCl}$ solution.

The current SAGE result [85] is $69 \pm 11_{-7}^{+5}$ SNU, and the current Gallex result [86] is $79 \pm 10 \pm 6$ SNU. The experiments are in good agreement (gratifying in view of the differences in method), with an average value of 74.3 ± 8.5 SNU, far below the standard-model prediction [71] of 132 ± 7 SNU. An intense artificial neutrino source (1.7 MCi of ^{51}Cr) has been used to verify the proper operation of Gallex; the ratio of observed to expected events was 1.04 ± 0.12 [87]. A similar test for SAGE is in progress.

9.2 Discussion of the Solar Neutrino Problem

The long-standing discrepancy between the measured rate in the Cl-Ar experiment and the predictions of astrophysical models engendered intensive experimental and theoretical work over the years to see if an explanation could be found within the framework of conventional physics. As a result, the “standard solar models” have been quite carefully checked with respect to both their conceptual framework and their experimental inputs. Small effects continue to be found, and the remote possibility of a gross, but still undetected, error, remains.

The MSW effect [52,63] can describe consistently the results of all four of the experiments [88,89,90,91,92,93]. Two allowed regions (see Figure 4) in oscillation space fit the data, within the framework of the standard solar model. An alternative particle physics solution is vacuum oscillations with large mixing ($\sin^2 2\theta \geq 0.6$) and small $\Delta m^2 \sim 10^{-10} eV^2$, for which the earth is at or near an oscillation node. This requires fine-tuning the earth-sun distance, but is otherwise marginally allowed [94,95]. Other solutions, such as neutrino decay [96] or large neutrino magnetic moments [97,98] are disfavored by the current data.

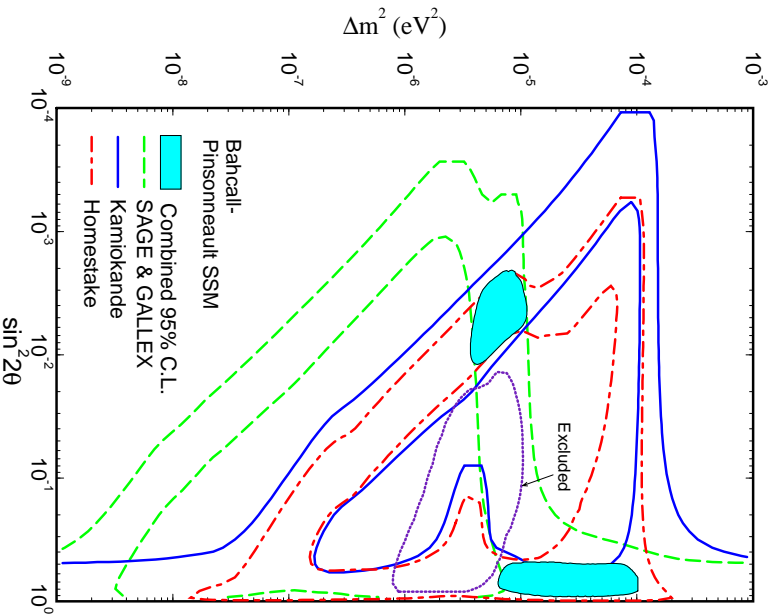


Figure 4: Allowed regions in $\Delta m^2 - \sin^2 \theta$ space for the four solar neutrino experiments and the Bahcall-Pinsonneault solar model. From [16].

The specific oscillation parameters derived depend on standard solar models (and, of course, contradict the Standard Model of particle physics). However, the existence of data from 3 distinctive spectral regions in 4 separate experiments invite us to distance ourselves from the detailed challenges of astrophysical theory. With a very limited set of assumptions, namely that the only type of neutrino emitted by the sun is the electron neutrino, and the only significant sources of such neutrinos are the pp and pep reactions, and the beta (or inverse) decays of ${}^7\text{Be}$, CNO isotopes, and ${}^8\text{B}$, one can ask if the total measured flux of neutrinos is consistent with the known power output of the sun. It is possible to address this

question without reference to detailed models because each termination in which 4 protons fuse to ${}^4\text{He}$ generates 26.732 MeV and precisely 2 electron neutrinos, independent of the reaction chain leading to termination. Some energy is carried away by the neutrinos, and is not available to heat the sun, but that ranges from 2.0% (PPI) to 6.4% (CNO). (The exception is terminations through ${}^8\text{B} - 26\%$ energy loss by neutrinos – but we know experimentally that that branch is orders of magnitude from playing a significant role in energy production.)

With current values for the experimental rates seen in the Cl-Ar, Kamiookande, and gallium experiments, one concludes that the total neutrino flux is (marginally) consistent (at about the 1.5σ level) with the elementary assumption set given, but that the ${}^7\text{Be} + \text{CNO}$ flux must be far smaller than calculated [64,65,66,67,68,69,70].

A particle-physics solution to the solar neutrino problem is therefore not absolutely required (yet), although there is manifest and unexplained inconsistency with “standard solar models.” This situation has been driven home by the gallium experiments, which were hoped to provide a clear decision for or against oscillations, but which have fallen in the “grey” region between forced particle-physics solutions and probable astrophysical solutions. To some degree, the fact that there is fair consistency with the total expected electron-neutrino flux tends to contraindicate a particle-physics solution. Elegant though the MSW mechanism is, it nevertheless is describing three data points with two parameters.

The solar neutrino problem does, however, suggest neutrino mass and oscillations by virtue of fundamental disagreement with astrophysical calculations, calculations that give a good account of many other solar parameters, such as the spectrum of mechanical oscillations of the sun and the Hertzprung-Russell diagram main sequence. The disagreement is not just in the difficult-to-calculate flux of ${}^8\text{B}$ neutrinos, but at the basic level that ${}^7\text{Be}$ seems to be almost absent in spite of the demonstrated presence of ${}^8\text{B}$, which can only be made from ${}^7\text{Be}$. No plausible astrophysical mechanism has been proposed to account for this. The possibility of failure of an experiment cannot be overlooked, but at least two of the three classes of experiment (chlorine, Kamiookande, gallium) would have to be in error [66,67,69] in addition to there being a failure in astrophysical theory. Final resolution of the issue must await new experiments that measure specific indicators of neutrino oscillations in a way independent of astrophysical models. New experiments are also of importance for astrophysics. With or without neutrino oscillations, they hold out the possibility of determining the initial neutrino flux components in a model independent way [65,66,68,69]. This and helioseismology are the only known direct probes of the solar core.

9.3 Forthcoming Experiments

9.3.1 The Sudbury Neutrino Observatory (SNO)

SNO is a neutrino detection facility sited at the 6800-foot level of the INCO nickel mine in Sudbury, Canada [99]. Built with support from four Canadian agencies, the US Department of Energy, and the UK Science and Engineering Research Council, SNO will consist of 1000 tons of 99.92%-enriched ultra-pure heavy water (D_2O) in an acrylic sphere surrounded by 7000 tons of light water as a shield.

Deuterium has unique nuclear properties that make it ideal for the study of neutrino interactions. There are four principal modes by which neutrinos can interact with heavy water:

$$d + \nu_e \rightarrow p + p + e^- - 1.44 \text{ MeV} \quad (27)$$

$$d + \nu_x \rightarrow p + n + \nu_x - 2.22 \text{ MeV} \quad (28)$$

$$d + \bar{\nu}_e \rightarrow n + n + e^+ - 4.03 \text{ MeV} \quad (29)$$

$$e^- + \nu_x \rightarrow e^- + \nu_x \quad (30)$$

The first of these reactions proceeds by the charged-current (CC) interaction of electron neutrinos specifically. The second is the neutral-current (NC) disintegration of deuterium and can be initiated with equal probability by any of the left-handed neutrinos (ν_e , ν_μ or ν_τ) and their antiparticles. The third is the charged-current interaction of electron antineutrinos (CA), which are not expected to be emitted from the sun except in certain very exotic scenarios. The fourth is the elastic scattering of neutrinos (ES). For each of these reactions, respectively, 9750, 5000, 0 and 1100 events per year are expected.

If neutrino oscillations occur, then the neutrinos may reach earth as other flavors. SNO therefore has the capability to reveal the presence of neutrino oscillations largely independent of solar properties. If the NC rate exceeds the CC rate (suitably normalized for cross sections), then neutrinos must be oscillating. If the CC energy spectrum differs from the known 8B spectrum, then neutrinos must be oscillating via the MSW mechanism [62,63], vacuum oscillations [94,95], the Voloshin-Vysotsky-Okun mechanism [97]ⁱ or neutrino decays [96], all of which predict different distortion patterns.

Unlike the kinematically convolved ES spectrum, the CC electron spectrum measured in SNO directly reflects the incoming ν_e spectrum (with quite good energy resolution) simply shifted down by 1.44 MeV. Being a real-time experiment, SNO will also be able to search for day-night differences due to regeneration in the earth (expected

for some regions of the MSW parameters) [100,101,102], and seasonal variations expected, for example, for vacuum oscillations [94,95]. SNO is a high-rate experiment. The interaction rates listed with the reactions above are for a 8B ν_e flux of $6 \times 10^6 \text{ cm}^{-2} \text{ s}^{-1}$, but no detection threshold. The NC threshold is the binding energy of the deuteron.

The Čerenkov light from charged-current and elastic-scattering events is detected in SNO by an array of 9,500 photomultipliers surrounding the acrylic sphere that holds the D_2O .

Neutral-current interactions on deuterium release a free neutron, and a number of strategies for detecting the neutron can be devised. One is to dissolve in the heavy water a fraction of a percent of chloride ion. When a neutron captures on 75% abundant ^{35}Cl , it emits an 8.6-MeV γ , which showers. The resulting Čerenkov radiation can be detected by the PMT array in the same way CC events are detected.

Another method is to detect the neutron in 3He proportional counters distributed in the heavy water so that the NC and CC events become completely distinct and no longer represent “backgrounds” to each other. One may also compare the ES rate with the CC rate to deduce the neutral-current contribution to the former. There are, then, 3 completely distinct methods for determining the NC rate, which will afford a check on systematic effects.

SNO will begin operation in 1996, and may provide a resolution of the solar neutrino problem.

9.3.2 SuperKamiokande

SuperKamiokande is a proton-decay detector with a total mass of 50,000 tons [77]. Like its predecessor, Kamiokande, ‘SK’ will also have solar-neutrino detection capabilities via the elastic scattering from electrons. However, the enormous fiducial mass (22,000 tons) means that, if the threshold can be brought down to 5 MeV, approximately 8,000 events per year will be recorded, 160 times more than with Kamiokande. A detailed measurement of the shape of the y -distribution can be made to see if the primary spectrum has been distorted by the MSW effect, time-dependent (day-night and seasonal) rates can be determined with precision, and an independent determination of the neutral-current rate can be made by comparison with the pure charged-current data from SNO (that can be done within SNO itself, but with much lower statistical precision). Any of those measurements can potentially provide model-independent evidence of neutrino oscillations.

SuperKamiokande is being constructed in Japan at the same depth as Kamiokande (3,000 mwe), and uses 11,300 50-cm photomultipliers plus 1,000 smaller tubes recovered from the IMB experiment in the veto. New electronics and careful control of radon will keep the

ⁱThe VVO mechanism and its variants [98] postulate a large magnetic moment (possibly excluded by other astrophysical effects [1]) to explain a possible anticorrelation of the Homestake rate with the sunspot activity. This has not been supported by the most recent data.

thresholds low. SK is scheduled for completion in 1996.

9.4 Experiments Under Development

9.4.1 Iodine

There is now under construction in the Homestake Mine an iodine solar neutrino detector. When fully completed, the detector will contain 100 tons of ^{127}I (225 tons total detector mass). The total solar neutrino detection rate of this detector should be fairly similar to that of the present chlorine detector at Homestake (135 tons of ^{37}Cl , 615 tons total). It is estimated [103] that the iodine detection rate per target nucleus is 4.5 times that of the chlorine detector. More importantly, the detection of neutrinos from ^7Be (see Table 4) by ^{127}I is almost half of the total rate, 14 SNU, while the detection rate for these neutrinos is only 1.1 SNU in the chlorine detector.

The fits to the neutrino flux measurements of the presently operating detectors indicate that the observed ^8B rate is about 40% of that predicted by the conventional solar model while that for ^7Be is less than 10% of the prediction. While it may be possible to reduce the predicted ^8B flux by modifications of nuclear input parameters and thus reduce or even eliminate the difference between predicted and observed neutrino fluxes, there have been no suggestions of any procedure that could significantly lower the expected ^7Be neutrino rate. Thus, the most critical present issue in the solar neutrino observations is the apparent absence of ^7Be electron neutrinos. It is generally assumed that this absence is an indication of neutrino flavor transitions, either in matter or in vacuum, into other neutrino flavors. Solar electron neutrino flux measurements with an iodine detector combined with those from the other detectors should be able to provide a clear measure of the electron neutrino flux from ^7Be in the sun. That, when combined with the multi-flavor neutrino measurements from Borexino, when that detector becomes operational, will then provide a measure of the non-electron neutrino flux from ^7Be , a crucial issue in searching for neutrino-flavor transitions.

The iodine detector will be modular with 10 tons of iodine per module. This modular structure permits fast extraction, 2 hours per cycle. Computer controlled extractions will be carried out daily at 6 a.m. and 6 p.m. The resulting ^{127}Xe will be stored in two charcoal traps, one for the daytime produced ^{127}Xe and the other for the nighttime produced ^{127}Xe . This procedure will permit a search for any day/night differences in the ^7Be neutrino flux caused by earth regeneration. In addition, since the detector will always be free of accumulated solar neutrino ^{127}Xe , it will always be fully sensitive to supernova signals.

All of the detector operating characteristics have been tested with one module of the detector. Construc-

tion of the full 100 ton, 10 module detector is now underway. The detector should be operational before the end of 1995.

A calibration program to determine the sensitivity of ^{127}I to ^7Be and ^8B neutrinos is also underway. The most readily available source of high-energy electron neutrinos is from the decay of stopped positive muons. The integral of the cross section for $^{127}\text{I} \rightarrow ^{127}\text{Xe}$ has been measured at LAMPF using the same radiochemical technique as that developed for the Homestake detector.

The ^7Be neutrino sensitivity can best be determined by calibrating the detector with a ^{37}Ar source. This source generates 814-keV neutrinos, very close to the 862-keV neutrinos emitted by ^7Be . Such a source can be produced in a reactor by fast neutron interactions on ^{40}Ca . It is also possible to determine the required matrix elements from the $^{127}\text{I}(p,n)^{127}\text{Xe}$ reaction.

9.4.2 Borexino

Present data indicate that a measurement of the ^7Be flux is of special interest. Astrophysical solutions would have to find a method to severely suppress the ^7Be flux, while MSW may convert most of the ν_e into ν_μ or ν_τ , which have an ES cross section 1/5 of the ν_e cross section. Some particle physics solutions predict a large time dependence. An Italian-US-German collaboration is carrying out the R&D necessary to construct a 100-tonne liquid-scintillator detector in Gran Sasso [104]. Extremely pure materials are required if radioactive backgrounds are not to mask the electron-scattering signal at 250 keV. No Čerenkov threshold protects the data from low-energy backgrounds in this experiment. A 4-tonne test detector is nearing completion. Given success, the INFN, NSF, and DFG will fund construction of the full-scale detector.

9.4.3 Icarus

A 5,000-ton liquid argon time-projection chamber is planned for Gran Sasso with a number of physics objectives including solar neutrinos. 'Icarus' can record both the elastic scattering from electrons and the charged-current inverse beta decay of ^{40}Ar to the isobaric analog state in ^{40}K , whose subsequent gamma decay provides a clear signature of the CC reaction. A 3-ton prototype has demonstrated the feasibility of drifting tracks 40 cm and reconstructing them [105].

9.4.4 Heron

A need to go to real time detection for the lower energy reactions (pp and ^7Be) requires the handling of events with energy depositions in the few-hundred-kilovolt range. The physical mechanisms for energy extraction (*e.g.*, phonons) in many materials at low temper-

ature would facilitate this. Because the fluxes are higher for these reactions detectors are expected to be of lower mass but significant complexity. They will require low temperature but low-power-capacity refrigeration. As in all solar neutrino detectors, extreme attention must be paid to backgrounds by shielding, implementation of distinctive event signatures, and radioactive purity of the target material and detector components. Helium is the purest material known with respect to radioactivity.

“HERON” (for Helium:Roton detection of Neutrinos) is a project under development by a group at Brown University which has invented a technique based on liquid helium in the superfluid state. The goal is to provide capability for a real-time detector with a threshold of 10 keV suitable for measuring the recoil-electron spectrum and rate from neutrino-electron scattering of both the pp and ${}^7\text{Be}$ neutrinos. A detector with a 10-ton fiducial volume would yield 18 events per day with the full standard-model flux of electron-neutrinos from those two sources.

In superfluid helium, energy transport out of the liquid can occur by ballistic propagation of rotons (phonons), evaporation of helium from the surface, and the subsequent detection of heat pulses on an array of bolometers above the liquid. The high multiplicity of rotons relative to ions is expected to be an important advantage in achieving a low threshold. Extensive tests of the detection method have been carried out by the Brown group using alpha, beta and gamma radioactive sources in a 3-liter prototype at 30 mK with a variety of bolometers. With 5-MeV alpha particles the details of the mechanism have been proven and sensitivity to event position and recoil direction established through a measured asymmetry in the radiated rotons. Energy, position and direction resolutions have not yet been measured for electrons; further work on electron detection and on bolometry is needed. The discovery that determination of recoil direction might be possible, a capability currently possessed only by the water Čerenkov detectors, is a significant development for studying the low energy solar neutrinos [106].

9.4.5 Hellaz

The contrasting approach utilizing gaseous helium under high pressure at low temperature (“Hellaz”) has been suggested to access the low-energy fluxes by a group from CERN/Collège de France/Gran Sasso/World Laboratory [107]. Two versions of a possible detector share a common basic technical implementation. A 20-ton mass of helium gas would be pressurized to 25 (or 50) atmospheres and held at 77 K. Operated as a time projection chamber, the detector cells would do pattern recognition as well as measure energy by track length and recoil-energy direction. The choice of TPC technology

precludes the use of liquid helium owing to its poor ion-drift properties. A successful application of the TPC method could be very powerful as a signature for solar neutrinos if the calculated energy and angle resolution can be achieved, and the radioactivity of the internal TPC hardware can be kept down. The basic physics processes are known but research is needed to provide laboratory evidence as to its feasibility, in view of the complexity of the device.

10 Atmospheric Neutrinos

Cosmic-ray interactions in the upper atmosphere produce pions and kaons whose subsequent decays produce a significant flux of neutrinos with energies below one GeV and moderate fluxes above this. Having traveled over path lengths of ≥ 20 km, these neutrinos are well suited for oscillation searches via the channel $\nu_\mu \rightarrow X$ in the range Δm^2 between 10^{-2} and 10^{-4} eV². There is much recent interest in the results of experiments measuring the flux of atmospheric neutrinos.^j The atmospheric neutrino flux is a mixture of approximately $\frac{1}{3}(\nu_e + \bar{\nu}_e)$ and $\frac{2}{3}(\nu_\mu + \bar{\nu}_\mu)$. It is therefore possible, in principle, to do both ν_μ and ν_e disappearance and appearance experiments. It is useful to define various classes of atmospheric neutrino interactions as follows:

- Fully contained events, with all tracks inside the fiducial volume of the detector.
- Partially contained events, which have the vertex inside the fiducial volume but at least one exiting track.
- Upward, stopping muons are produced from neutrinos interacting outside the detector, and contain a muon which stops inside a fiducial volume.
- Upward, throughgoing muons are also from external neutrino interactions but the muons pass through the detector, producing than some minimum track-length inside a fiducial volume.

Low statistical precision limits the reach in $\sin^2 \theta$, while the neutrino energy (E_ν) and the earth’s radius (R_{earth}) limit the reach in Δm^2 of neutrino oscillation experiments with the atmospheric neutrino flux. Uncertainties in normalization of the primary cosmic rays, together with uncertainties in the production of pions and kaons in proton collisions with light nuclei, translate into significant uncertainties in the normalization and shape of the atmospheric neutrino spectrum at production. For this reason, conclusions based on ratios are safest.

10.1 Current Status

10.1.1 Contained Events

The neutrino flavor ratio from experiments [108,109] which measure contained events is shown in Table 5,

^jThis section is based on materials prepared by T. Gaisser, Bartol Research Institute and M. Goodman, Argonne National Lab.

Table 5: The atmospheric neutrino flavor ratio from various experiments. R' is defined in the text.

| Experiment | Exposure kT-year | R' |
|-------------------------------------|---------------------|--------------------------|
| IMB1 | 3.8 | 0.68 ± 0.08 |
| Kamiokande ring | 7.70 | $0.60 \pm 0.06 \pm 0.05$ |
| Kamiokande decay | | $0.69 \pm 0.06 \pm 0.05$ |
| IMB-3 ring | 7.70 | $0.54 \pm 0.05 \pm 0.05$ |
| IMB-3 decay | | $0.69 \pm 0.06 \pm 0.07$ |
| Fréjus contained | 2.0 | $0.87 \pm 0.13 \pm 0.07$ |
| Soudan 2 | 1.01 | $0.64 \pm 0.17 \pm 0.09$ |
| NUSEX | 0.5 | 0.99 ± 0.29 |
| <i>Uncontained events included:</i> | | |
| Kamiokande Multi-GeV | 7.70 | $0.57 \pm 0.08 \pm 0.07$ |
| Fréjus total | 2.00 | $1.00 \pm 0.15 \pm 0.08$ |

while the data and calculations themselves are shown in Table 6. The flavor ratio is

$$R \equiv \frac{(\nu_\mu/\nu_e)^{data}}{(\nu_\mu/\nu_e)^{MC}}, \quad (31)$$

while the experiments actually measure

$$R' \equiv \frac{(track/shower)^{data}}{(track/shower)^{MC}}. \quad (32)$$

These only differ if there are neutrino oscillations in the presence of neutral current backgrounds to the track and shower samples. Systematic errors in Table 6, where shown are added quadratically. IMB has shown their systematic errors added linearly [110].

The high-statistics water Čerenkov detectors in Table 5 have two ways to distinguish quasi-elastic ν_μ and ν_e events. In one method, the shape of the Čerenkov ring on the wall of the phototubes is used. In the other method, excess phototube hits in a window several microseconds after the event indicate μ or π decay. The two methods have different systematic errors, but are statistically correlated. Experimental tests of e/μ detection efficiency are underway at KEK. Results from the Kamioka group presented at Eilat [111] show no sign of misidentification. Results from the IMB exposure at KEK can be expected in 1995. The Fréjus experiment prefers to analyze their contained and partially contained events together. This is discussed in the next section.

The results on contained atmospheric neutrino events are consistent with each other, and with a 30-40% deficit of ν_μ events. Such a deficit could be the result of either $\nu_\mu \leftrightarrow \nu_\tau$ or $\nu_\mu \leftrightarrow \nu_e$ oscillations. Since the interpretation of the atmospheric neutrino anomaly in terms of neutrino oscillations depends on the normalization of the neutrino flux, it is desirable to check the normalization as well as possible. In a conventional two-detector

Table 6: The data and Monte Carlo predictions on the atmospheric neutrino deficit from several experiments. TR refers to single tracks, SH to single showers.

| Experiment | TR^{see} (ν_μ^{see}) | TR^{MC} (ν_μ^{MC}) | SH^{see} (ν_e^{see}) | SH^{MC} (ν_e^{MC}) |
|------------------|-----------------------------------|---------------------------------|---------------------------------|-------------------------------|
| IMB1 | 104 | 136 | 297 | 265 |
| Kam. ring | 234 | 356.8 | 248 | 227.6 |
| Kam. decay | 182 | 277.5 | 300 | 313.9 |
| IMB-3 ring | 182 | 268 | 325 | 257.3 |
| IMB-3 decay | 208 | 261.5 | 402 | 348.5 |
| Fréjus contained | 94 | 100 | 89 | 82 |
| Soudan 2 | 33.5 | 42.1 | 35.3 | 28.7 |
| NUSEX | 32 | 36.8 | 18 | 20.5 |

neutrino oscillation experiment, this is done by measuring the interaction rate in the neutrino beam close to the source. The nearest analog for the atmospheric neutrino beam of a close-in detector is a measurement of the intensity of muons at the same altitudes where both the neutrinos and muons are produced (10 to 20 km). New, higher precision measurements of this flux are being made [112,113], and preliminary results [112] are consistent with a relatively high normalization of the neutrino flux [114]. This favors an interpretation of the atmospheric neutrino puzzle in which ν_μ disappear, rather than transform into ν_e . (Note that the neutrino energies are below τ production threshold.)

10.1.2 Partially Contained Events

The most recent new result on atmospheric neutrinos is the Kamiokande analysis of their “multi-GeV” events, which include fully contained events with $E_{vis} >$

1.33 GeV as well as partially contained events [115]. The mean neutrino energy responsible for this latter class of events is ~ 6 GeV. This is nearly an order of magnitude higher than for the independent sample [116] of contained events with $E_{\text{vis}} < 1.33$ GeV. In this new data sample, there is again evidence for a ν_μ deficit, with a measurement of $R' = 0.59 \pm 0.08$.

The most remarkable feature of the data is the appearance of an angular dependence of the muons of the kind that would be expected if downward muons have path-lengths too short to oscillate; that is, the upward muons are suppressed relative to the downward muons. Given the range of E_ν and R involved for the multi-GeV sample, Eq. (22) implies an upper limit on Δm^2 . In contrast to the muons, the angular dependence of the electrons is closer to what is expected if the ν_e are not affected by oscillations. The angular-dependence alone therefore suggests an interpretation in terms of ν_μ disappearance.

On the other hand, a preliminary re-analysis of the Fréjus data presented at Snowmass [117] seems to be even more divergent from the Kamiokande and IMB results of Refs. [116,118] than the original Fréjus publication [119]. A simultaneous analysis of their contained, partially contained, and throughgoing muons leads to a neutrino oscillation exclusion plot which contradicts a neutrino oscillation interpretation of the data in Tables 5 and 6. The Fréjus fully contained data are not, by themselves, in strong disagreement with the other experiments. However, their partially contained events and neutrino induced throughgoing muons seem to be in conflict with the new Kamiokande result. An analysis of all Fréjus neutrino data leads to the result $R' = 0.96 \pm 0.18$.

One puzzling feature of the new Kamiokande result is that there appears to be a large excess of electron neutrinos and a relatively small deficit of muon neutrinos as compared to the calculation. Using the neutrino flux of Ref. [120], they find

$$e\text{-like} \left(\frac{\text{measured}}{\text{calculated}} \right) = 1.47 \pm 0.15 \quad (33)$$

and

$$\mu\text{-like} \left(\frac{\text{measured}}{\text{calculated}} \right) = 0.83 \pm 0.07. \quad (34)$$

The corresponding numbers for the low-energy, fully contained event sample are 1.09 (electrons) and 0.66 (muons). Thus, while the low energy sample suggests $\nu_\mu \leftrightarrow \nu_\tau$, the high-energy sample looks more like $\nu_\mu \leftrightarrow \nu_e$.

10.1.3 Upward Stopping Muons

The measured ratio of stopping to throughgoing upward neutrino-induced muons is consistent with expectation [121]. The data are shown in Table 7. This means *either*

that there are no oscillations of ν_μ with mixing angle and Δm^2 large enough to be seen with upward neutrinos *or* that there may be large mixing of ν_μ , but with Δm^2 large enough so that the lower energy stopping muons as well as the higher energy throughgoing muons are affected. The measured stopping/throughgoing ratio is used to rule out a range of $10^{-3} < \Delta m^2 < 10^{-2}$ eV² at large mixing angle for ν_μ disappearance [121].

The ratio of upward stopping muons to throughgoing muons is sensitive to the absence of background from events that are not initiated by neutrinos. In particular, downgoing muons which initiate hadronic cascades in the rock could mimic upward going stopping muons in some cases. There is evidence for such events from Soudan, Kamioka, and MACRO [122,123,124], but it is not straightforward to calculate the possible contamination of the IMB data sample. A background of 12 events out of the 85 would lead to the absence of any neutrino oscillation limit from the IMB analysis. A comparison of upward showers to expectation in IMB may be evidence that such a background in fact exists.

Table 7: Neutrino induced upward event rates in IMB.

| | Observed | Calculated |
|-----------------|----------|------------|
| Stopping tracks | 85 | 84 |
| Exiting tracks | 532 | 516 |
| Showers | 49 | 17 |

10.1.4 Upward Muons

The implications of upward muon measurements have been somewhat controversial. The IMB group [121] calculated the rate of upward, throughgoing muons assuming a particular neutrino flux [125] and a particular representation of the neutrino cross section [126]. Their calculated rate agreed with their measured rate, apparently ruling out most of the available parameter space needed for a ν_μ -disappearance interpretation of the low energy, contained event anomaly. Frati *et al.* [127] showed that the Kamiokande data on upward, throughgoing muons [128] is similarly consistent with a calculation assuming the same input. On the other hand, they found that, starting from different, more recent calculations of the neutrino flux [129,130] and a different representation of the cross section [131], the predicted rate is some 15% higher than the observed rate. They further showed that a discrepancy of this size is consistent with a range of parameters needed to explain the contained event anomaly as ν_μ -disappearance. Recently reported results from MACRO [132] similarly show a significant deficit of the measured upward rate as compared to a calculation with the “high” input assumptions. This ma-

trix of measurements and calculations is indirect evidence that these experiments are all consistent. The same cannot be said for Baksan [133] where there is agreement between measurement and expectation for “high” input assumptions, but an *excess* of measurements over calculation when the low input is used. In all cases the differences are only of marginal statistical significance, as indicated by the summary of measurements/calculations in Table 8.

Table 8: Upward muons. For Kamioka the units are upward muons in units of $10^{-13} \text{cm}^{-2} \text{s}^{-1} \text{sr}^{-1}$. For IMB, upward events per day and for Baksan and MACRO total number of observed upward events.

| Experiment | Observed | Calculated | |
|--------------|------------------|--------------|-------|
| | | “high” | “low” |
| IMB [121] | 0.47 ± 0.02 | — | 0.455 |
| KAM [128] | 2.04 ± 0.13 | 2.36 | 2.18 |
| Baksan [133] | 161 | 162 | 142 |
| MACRO [132] | $74 \pm 9 \pm 8$ | 101 ± 15 | — |

10.1.5 Summary of Atmospheric Neutrino Data

Experiments with atmospheric neutrinos can be ranked in the order of their potential for discovery of new physics as follows:

1. Measurements of the ratio ν_e/ν_μ . Here, the principal uncertainties in the input to the calculation of this ratio all cancel. Three completely independent calculations [134,120,135] for the expected value of this ratio agree among themselves within 5%.
2. Angular distributions of neutrino fluxes in a particular energy region. Again, the principal uncertainties cancel in the calculation, but the statistical significance is poorer because the data must be subdivided into angular bins.
3. The ratio of stopping to throughgoing neutrino-induced upward muons. The cancellation of uncertainties in the calculations here is less complete because the two classes of events in this ratio correspond to different ranges of energy.
4. The absolute intensity of ν_μ or ν_e .

It is noteworthy that the experiments with the greatest statistical significance [116,118] show a significant deviation from the most secure feature of the atmospheric neutrino beam—the ν_e/ν_μ ratio. The measured value is apparently greater than the ratio at production. The possibility that the discrepancy might result from an

oversimplified use of the Fermi Gas Model (FGM) in calculating the neutrino interaction rate is not borne out by careful investigations [136], which conclude that the energy is high enough that any deviation from the FGM affects both flavors of neutrinos similarly. On the other hand, recent reports from the Los Alamos LSND experiment indicate that the ν_μ cross section on ^{12}C is a factor 3 below FGM expectations while the ν_e cross section is not. The energies in this experiment, however, are considerably lower than those relevant to the atmospheric neutrino signal.

If the observed effect is a signal of neutrino oscillations, the lack of observed angular dependence for low energy ($\lesssim 1 \text{ GeV}$) events [116,118] implies $\Delta m^2 > 10^{-3} \text{ eV}^2$. The large size of the discrepancy requires $\sin^2 2\theta > 0.5$. Much, but not all, of the available phase space for a $\nu_e \leftrightarrow \nu_\mu$ explanation is ruled out by reactor limits. New long-baseline reactor experiments at San Onofre and Chooz are under construction to close the gap completely (see Section 11).

A ν_μ disappearance interpretation (*e.g.*, $\nu_\mu \leftrightarrow \nu_\tau$) of the ratio ν_e/ν_μ in low-energy contained events with $\Delta m^2 > 10^{-2} \text{ eV}^2$ and large mixing angle would imply disappearance of $\sim 100 \text{ GeV}$ ν_μ with path-lengths $L > R_{earth}$. This in turn predicts a deficit of ν_μ -induced, upward, throughgoing muons. Measurements of this rate are inconclusive because of uncertainty in the normalization of the calculated neutrino flux. There is also some uncertainty in the neutrino cross section. Combining all their data (sub-GeV and multi-GeV), the Kamiokande group find a rather limited allowed region, either for $\nu_\mu \leftrightarrow \nu_\tau$ or for $\nu_\mu \leftrightarrow \nu_e$ with nearly full mixing and with $\Delta m^2 \sim 1 \text{ to } 2 \times 10^{-2} \text{ eV}^2$. Simultaneous analysis of all atmospheric and solar neutrino data sets (as of 1993) in the space of 3-flavor neutrino oscillations [137] favors oscillation predominantly in the $\nu_\mu \leftrightarrow \nu_\tau$ sector to explain the atmospheric^k and in the $\nu_\mu \leftrightarrow \nu_e$ sector for the solar neutrinos. This in turn implies a “natural” order for the neutrino masses, with $m_{\nu_\tau} \sim 0.1 \text{ eV}$ and $m_{\nu_\mu} \sim 0.003 \text{ eV}$.

10.2 The Next Five Years

Between now and 1999, Soudan 2’s exposure will grow from 1.8 to 5.0 kt-years. The present result, 0.69 ± 0.19 (based on 1.0 kt-year) could change to 0.69 ± 0.08 or 1.0 ± 0.12 . The low value would confirm the deficit in a detector with much different systematic errors. However, compared to 14 kt-years of present Čerenkov detector data, neither Soudan answer would resolve the situation. Systematic studies of a water Čerenkov detector using IMB and Kamioka photomultiplier tubes are taking place

^kOscillations into sterile neutrinos are disfavored by nucleosynthesis. See Section 3.

in a KEK test beam. This will check their thresholds, efficiencies, and pattern recognition capabilities. In 1996, Superkamiokande (see Section 9.3.2) will take data and, in another year or two, these data will compete statistically with the present world sample. Since the muon neutrino deficit is unlikely to be due to a statistical fluctuation, this may not resolve the situation either. The angular distribution of contained events and Multi-GeV events in Superkamiokande might provide additional evidence concerning an oscillation interpretation for values of Δm^2 below $\sim 10^{-2} \text{ eV}^2$.

If the atmospheric neutrino deficit is an experimental artifact, it is hoped that the cause can be identified in the next few years. However, if the cause is neutrino oscillations, the evidence may be limited to the anomalous flavor ratio and low statistics angular distributions unless new atmospheric or accelerator experiments are built.

10.3 Beyond 1999

Three new detector projects have the potential to bring atmospheric neutrinos to the realm of a high statistics and well measured field of study during the first decade of the 21st century. These are the ICARUS high resolution Argon drift chamber for the study of contained events, a large new underground long baseline neutrino detector for the study of semi-contained events and upward stopping muons, and a km^3 array in water or ice for the study of throughgoing neutrino induced muons. In addition, the phenomena can be studied directly in long baseline accelerator experiments, as discussed in Section 12.

10.3.1 ICARUS

The ICARUS collaboration plans to build a 5-kiloton liquid-argon projection chamber in the Gran Sasso Laboratory. As they have demonstrated with a 3-ton prototype, such a detector would have unprecedented pattern recognition capabilities for atmospheric neutrinos. The technique can provide a high electron to muon discrimination for both quasi-elastic and deep inelastic atmospheric neutrino events, a precise energy measurement, a good neutrino direction reconstruction, and a partial neutrino to antineutrino separation (by means of the different capture to decay ratio for μ^+ and μ^- in argon.) With about 4 kT-yrs per year of fiducial exposure, this should provide dramatic confirmation if the atmospheric neutrino anomaly is due to oscillations.

10.3.2 Long Baseline Detector Capabilities for Atmospheric Neutrinos

The motivation and capabilities of long baseline neutrino detectors will be discussed in the next section. However,

a 15 kTon underground magnetized detector, such as envisaged for a Fermilab or CERN experiment, would be a new powerful tool in understanding the semi-contained atmospheric neutrinos. The magnetic field would allow the charge ratio to be measured unambiguously, and good timing would allow separation of semicontained neutrino interactions from other cosmic-ray backgrounds. The combination of measuring the hadron shower in the calorimeter, and the muon momentum with the magnetic field, would allow the full reconstruction of atmospheric charged-current neutrino events. If the neutrino-oscillation interpretation of the atmospheric anomaly is correct, there would be many new signals that could be confirmed in such detectors.

10.3.3 Cubic Kilometer Neutrino Detectors

IMB measured the upward going muon flux with an effective area around 300 m^2 . Kamioka, Baksan and Soudan 2 have similar effective areas, while MACRO is larger. However a square kilometer effective area (as part of a cubic kilometer detector) would measure the flux and angular dependence of the upward going muons with 3000 times the present statistics. The DUMAND, NESTOR, AMANDA and Lake Baikal collaborations are providing the first generation of large underwater or deep ice experiments. To date, none of them have been able to separate atmospheric neutrino induced muons from the cosmic ray backgrounds. But each has overcome considerable technical obstacles, and hope to demonstrate feasibility of deep water/ice muon detection and directionality soon. If further economies of scale can be shown to exist in the course of those studies, a km^3 detector could be planned for ten years from now. As discussed above, very high statistics measurement of the angular distribution of neutrino induced muons would be sensitive to large neutrino mixing over a wide range of Δm^2 .

11 Reactor Neutrinos

Since the discovery of the electron antineutrino by Reines and Cowan in 1956, reactor neutrino experiments^l have continued to provide an essential tool in the elucidation of the properties of the neutrino.

The nuclear β -decay of the fission products of nuclear reactors produce a very large flux of low energy (up to $\sim 8 \text{ MeV}$) $\bar{\nu}_e$'s. This allows for a study of the disappearance channel $\bar{\nu}_e \rightarrow X$. One can search for oscillations by measuring the energy spectrum of antineutrinos at a distance, L , from their source and comparing with expectations. The occurrence of oscillations will cause this spectrum to be modified from the predicted "no oscillation" spectrum. Such a measurement is non-trivial

^lThis section is based on material prepared by Richard Steinberg, Drexel University.

since the comparison depends on understanding the initial spectrum, which depends on the yields of each of the fission products. Uncertainties in the calculations which lead to these predictions limit the ultimate accuracy. One method to reduce the uncertainties involves comparing neutrino yields at two or more distances from the reactor source. In most reactor experiments, neutrinos are detected using the charged current reaction $\bar{\nu}_e + p \rightarrow e^+ + n$. The signature for this reaction is a time correlated pair of positron and neutron signatures.

11.1 Current Status

The current best limits for neutrino-oscillation parameters from reactor neutrino experiments are derived from a generation of experiments using detectors of several hundred kilogram mass at distances up to about 100 meters from the source. Although these distances are relatively short compared to those possible with accelerator neutrino experiments, the L/E ratios are more than competitive.

The lower energies, together with excellent understanding (at the level of $\sim 2\%$) of the initial neutrino flux spectrum and flavor composition, permit the reactor neutrino oscillation experiments to provide convincing information about neutrino oscillations in an interesting region in the space of Δm^2 vs $\sin^2 2\theta$. The current limits from reactor experiments at both the Gosgen and Bugey reactors rule out neutrino oscillations involving electron neutrinos to a Δm^2 level of 10^{-2} eV^2 at maximal mixing, and to $\sin^2 2\theta$ values greater than about 0.05 for large Δm^2 .

11.2 Experiments Under Construction

The continuing puzzle with respect to solar neutrinos together with an apparent anomaly in the atmospheric neutrino fluxes has stimulated interest in a new generation of reactor neutrino experiments. Two of the proposed experiments have been approved and are now under construction. The sensitivity of each will completely cover the region of parameter space indicated by the atmospheric neutrino anomaly and extend down to the level of $\Delta m^2 = 10^{-3} \text{ eV}^2$.

Both experiments will utilize a gadolinium-loaded liquid scintillator neutrino target of about 5-10 tons mass located about one kilometer from a large nuclear power station. The reaction to be measured is the classic Reines-Cowan inverse β -decay reaction, $\bar{\nu}_e + p \rightarrow e^+ + n$. Neutrino oscillations coupling $\bar{\nu}_e$ to any other neutrino would be inferred from the $\bar{\nu}_e$ disappearance.

The first and most sensitive method for extracting the signal would be an absolute comparison of the measured integrated count rate with the rate calculated from

knowledge of the neutrino source and of the absolute detector efficiency.

An additional signature for neutrino oscillations would result from the study of distortions in the measured positron spectrum. In certain regions of the parameter space, this study could lead to a very clear, perhaps unmistakable signature for neutrino oscillations.

The detector design philosophies in the two experiments, however, are quite different. This situation is fortunate, since the different systematic effects in the two detectors should provide an extra measure of confidence in any jointly observed result. History teaches that this approach is indeed wise.

The San Onofre experiment [138] is being performed by a collaboration of groups from Caltech, the Institute for Nuclear Research (Moscow) and Stanford University. The experiment will be located at the depth of 25 meters water equivalent (mwe). To reduce the substantial cosmic ray-induced backgrounds at this depth, a segmented detector design was developed, utilizing a three-fold prompt coincidence signature for the positron, together with a delayed coincidence requirement for the positron-neutron capture sequence. The price paid for the complex geometry and coincidence requirements is a relatively low overall efficiency of about 20% as well as substantial difficulty in precise determination of the absolute detector efficiency.

The Chooz Experiment [139,140] is being performed by a collaboration of groups from Annecy, the Collège de France, Drexel University, the Kurchatov Institute, Pisa, Trieste, and the Universities of California (Irvine) and New Mexico. The experiment utilizes a site one kilometer from an 8.2 GW nuclear power station nearing completion in northern France. The site was selected because of its substantial underground depth of 300 mwe. With a 200-fold cosmic-ray rate reduction provided by the overburden, an unsegmented nearly-spherical detector design was adopted. The efficiency of the detector for positrons from neutrino inverse beta decay events is above 80% and relatively easy to model and to calibrate.

Each of the experiments expects to begin data taking before the end of 1995.

11.3 The Future

Future work on neutrino oscillation studies with reactor neutrinos could be aimed in at least three complementary directions.

Improvement of our knowledge of the reactor neutrino spectrum would allow improved sensitivity to small values of $\sin^2 2\theta$. This direction may be especially appropriate as a means to verify results from the LSND experiment discussed in Section 12. Sensitivity to mixing angles as small as 1% would be a reasonable goal.

A second opportunity for further work would be to

improve the sensitivity of the long baseline reactor experiments to smaller values of Δm^2 . It has been suggested that it is possible to extend the basic technique of the Chooz experiment to neutrino baselines of at least ten kilometers [141,142]. With such an experiment, which would require a deep underground site and a kiloton-scale detector, sensitivity to Δm^2 lower than 10^{-4} eV² can be reached. The decision whether to pursue such an experiment probably should await the results of the present generation of one-kilometer neutrino oscillation experiments.

Finally, one should explore and encourage the possibility of using other neutrino reactions, such as neutral- and charged-current reactions in deuterium to provide sensitive oscillation tests.

12 Accelerator Neutrinos

The regions of parameter space which appear “interesting” because of the outstanding questions of dark matter and atmospheric neutrinos extend just beyond the reach of completed first generation accelerator experiments. This tantalizing situation has recently spurred a renewed interest in accelerator based searches and led the way to a second generation, some of which are currently operational and will take data in the near future. In this section we will review the status of on-going experiments and discuss options for new initiatives to significantly extend the reach in parameter space.

12.1 Large Δm^2

12.1.1 The $\nu_\mu \rightarrow \nu_e$ Channel

LSND The LSND experiment at Los Alamos is searching for $\nu_\mu \rightarrow \nu_e$ and $\bar{\nu}_\mu \rightarrow \bar{\nu}_e$ oscillations using muon neutrinos produced in the decay of pions produced by the LAMPF proton beam. A signal in their detector, composed of 200 tons of dilute liquid scintillator which is sensitive to the appearance of low energy electrons, would indicate the occurrence of a ν_e ($\bar{\nu}_e$) charged current interaction resulting from the oscillation of $\nu_\mu \rightarrow \nu_e$ ($\bar{\nu}_\mu \rightarrow \bar{\nu}_e$). Preliminary reports suggest that such signals are indeed seen, with strong statistical significance in the $\bar{\nu}_\mu$ channel[143]. The regions of parameter space in which an oscillation may be indicated is for Δm^2 of a few eV², and $\sin^2 2\theta \sim 10^{-2}$.

KARMEN The KARMEN experiment is also sensitive to the $\bar{\nu}_\mu \rightarrow \bar{\nu}_e$ channel. KARMEN is a 56 ton liquid scintillator calorimeter which like LSND, measures neutrinos from a beam dump for 800 MeV protons from the ISIS storage ring at Rutherford Laboratory. The experiment has been taking data for four years and anticipates a further two years of data taking. At the present time

the experiment does not report any significant number of events above the expected background[144].

12.1.2 The $\nu_\mu \rightarrow \nu_\tau$ Channel

The recently renewed realization that tau neutrinos may play a critical role in cosmological dynamics has revived interest in searching for $\nu_\mu \rightarrow \nu_\tau$ oscillations for mass differences in the 5-100 eV range. This search, when done with a definitive “appearance” experiment, requires intense primary proton beams with energies above 100 GeV but only “short” baselines, *i.e.*, of less than a kilometer. These parameters are ideally suited for carrying out (relatively inexpensive) oscillation searches at Fermilab and CERN.

Tau neutrino appearance experiments are designed to detect the τ lepton from ν_τ interactions, either by direct observation of a short-lived τ track and kinematic information, or by use of kinematic information alone. These highly-instrumented but relatively low-mass detectors have high sensitivity (ultimately, a few times 10^{-5}) in $\sin^2 2\theta$ for $\nu_\mu \rightarrow \nu_\tau$ oscillations because of their excellent background rejection. Sensitivity to $\nu_e \rightarrow \nu_\tau$ is typically a factor 50-100 worse because ν_e is a minority component in accelerator-produced beams. (Fortunately, the ν_τ content of such beams is negligible.) These experiments have maximum sensitivity in the mass range which is cosmologically interesting. However, with short baselines they cannot access Δm^2 below a few tenths of an eV², even at maximum mixing.

The CERN Laboratory is now beginning a new generation of $\nu_\mu \rightarrow \nu_\tau$ oscillation experiments, CHORUS [145] and NOMAD [146], that promise to extend the relevant mixing-angle sensitivity an order of magnitude by identifying one or more channels of tau lepton decay.

CHORUS The first experiment, CHORUS, will use a hybrid emulsion spectrometer to directly search for the production of τ leptons from ν_τ charged current interactions. The distance of the detector from the proton target (~ 800 m) and the average beam neutrino energy makes the experiment sensitive to tau neutrino mass as low as 1 eV. Limits in the mixing angle between tau and muon neutrinos have been measured previously (in this range of masses) by the Fermilab E-531 experiment[147] at the level of $\sin^2 2\theta = 4 \times 10^{-3}$. The CHORUS experiment expects to improve this limit by a factor 10. For an integrated intensity of 2.4×10^{19} protons on target about 500,000 muon neutrino interactions are expected. This should be achievable over two calendar years.

NOMAD The second experiment, NOMAD, will attempt to identify the occurrence of τ production by the kinematic distribution of particles produced in the interaction. Unlike CHORUS, which has the ability to defini-

tively identify the tau track, NOMAD, relies totally on the signature of missing transverse momentum. Hence, to make a case that a signal has been seen, it will be crucial to demonstrate that the missing transverse momentum is not due to other sources. The NOMAD experiment will measure the momentum of charged particles by tracking them in a magnetic field, and will measure the momentum of photons with a preshower and lead glass electromagnetic calorimeter. A hadronic calorimeter is also being added to the experiment.

Data taking began with the new CERN wide band neutrino beam in April 1994, and ended in October 1994. After a several-month hiatus data taking will resume and continue until the end of 1995. Further data taking in 1996-97 has been approved.

FNAL E-803 In early discussions of the Fermilab Main Injector project it was realized that this new machine would provide the opportunity to produce a very high-intensity, moderate energy neutrino beam. A beam of 120 GeV protons could be extracted at least every two seconds at an intensity of $3\text{-}6 \times 10^{13}$ protons per pulse. In 1990 the first proposal submitted to the Laboratory to use such a beam, E-803 [148], proposed to use a high-resolution hybrid emulsion spectrometer to do a definitive tau appearance experiment. Delays in the approval of the Main Injector project resulted in a several-year deferral of serious consideration of E-803. In the meantime the opportunity to do a similar experiment at CERN (discussed above) was proposed and approved. The major difference between CHORUS and E-803 is in E-803's significantly greater resolution for actually identifying τ decays. In contrast to the CERN experiments which emphasize the $\mu\nu\bar{\nu}$ and the $e\nu\bar{\nu}$ modes, E-803 will concentrate on the ability to identify τ decays in the two-body and quasi-two-body modes $\pi^-\nu$ and $\rho^-\nu$ (with $\rho^- \rightarrow \pi^-\pi^0$), which have distinctive kinematic signatures and measurable proper decay times. E-803 was approved in November 1993. As will be discussed below, the present Fermilab plan is to perform E-803 in conjunction with a long-baseline experiment, hence maximizing the reach into parameter space with a single neutrino beam. In the absence of a signal, E-803 would extend the limits in mixing angle by a factor of five to ten over the CHORUS experiment at very large Δm^2 , and by more than a factor of thirty at values of Δm^2 in the few electron volt range. These limits are summarized in Figure 5.

FNAL E-872 Though there is a great deal of evidence that the ν_τ exists as a unique lepton and that its couplings are not anomalous at the present level of sensitivity, interactions of ν_τ have yet to be observed, as have those of the ν_e and ν_μ . To accomplish this, an experiment requires high proton intensities, high energy, and

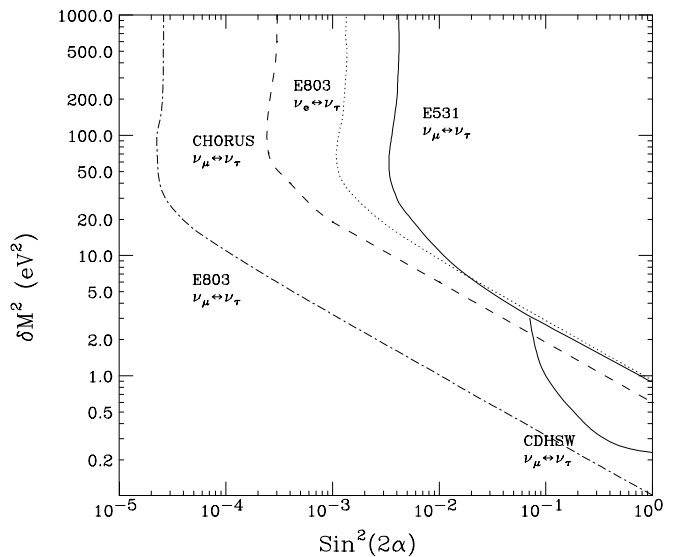


Figure 5: Present limits in the channel $\nu_\mu \rightarrow \nu_\tau$, as well as those expected from the on-going CHORUS experiment, and the E-803 experiment.

extremely good detector resolution. The Fermilab Tevatron in conjunction with a high resolution hybrid emulsion spectrometer meets these requirements. A newly approved experiment, E-872, will produce τ neutrinos in a beam dump and directly measure ν_τ charged current interactions by seeing τ decays in an emulsion target using the same hybrid emulsion technique as CHORUS and E-803. This experiment will be performed during the 1996-97 Fermilab fixed-target run prior to the completion of the Main Injector. E-872 should see the interaction that the oscillation experiments hope to see, if the ν_τ is "standard". E-872 will be also be sensitive to and measure the processes that give rise to backgrounds for the experiments seeking ν_τ oscillation.

12.2 Extending the Search to Small Δm^2

Conceivably, neutrinos could have the small, non-zero masses and relatively large mixing angles suggested by the apparent deficit of atmospheric muon neutrinos. Definitive "disappearance" experiments can be carried out at a number of accelerator laboratories to test this hypothesis directly. Such experiments require intense neutrino beams and at least two detectors separated by tens to hundreds of kilometers, depending on the neutrino energy and the difference in neutrino masses that is being explored. Long base-line "disappearance" experiments require careful detector alignments and neutrino flux measurements. They tend to be relatively expensive because of the required infrastructure (downward-sloping beams, two detectors with the far one containing a large target mass). However, they represent a unique oppor-

tunity to discover neutrino oscillations in the range from about 10^{-3} to several eV in a controlled laboratory setting.

In the following subsections we will briefly discuss several proposals for accelerator based long-baseline oscillation searches. Reactor searches were described in Section 11.

12.2.1 $\nu_\mu \rightarrow \nu_e$ and $\nu_\mu \rightarrow X$

BNL The Brookhaven AGS has a long history of providing high intensity proton beams which are then used to produce high flux beams of neutrinos. Present plans to increase the intensity of the AGS by a factor of four, to 6×10^{13} protons per AGS cycle of 1.6 sec, have made it possible to consider extending the oscillation search into the small Δm^2 region as well [149].

In Spring 1993, the Brookhaven AGS PAC recommended physics approval for P899, a *Proposal for a Long Baseline Neutrino Oscillation Experiment at the AGS*. The principal aim of the experiment is to explore the region of parameter space suggested by the atmospheric neutrino deficit. The experiment would use a neutrino beam produced by the 26 GeV protons from the AGS. The average neutrino energy would be about 1 GeV, which is similar to the energies of cosmic neutrinos which show evidence for oscillations. By placing detectors at several locations (1, 3 and 24 km), the disappearance of neutrinos (and possibly the appearance of ν_e) in the mass region of a few 10^{-3}eV^2 will be detectable if the mixing is relatively large. For an integrated delivered proton intensity of $\sim 2 \times 10^{20}$ protons, more than 4000 contained muon events should be detectable in the far detector. As proposed, the far detector would be located in a tank farm on the north shore of Long Island. To produce a neutrino beam in this direction will require construction of a new proton transport line from the AGS. The detectors for E899 are identical, massive water Cerenkov detectors, 15 meters in diameter by 15 meters in height. Each tank will contain 1900 20-cm diameter photomultiplier tubes.

As of late 1994, the E899 collaboration was preparing an upgraded proposal. In addition to the detectors at 1, 3, and 24 km, as originally proposed, a fourth detector site consisting of two additional tanks is proposed at a distance of 67 km, to be located at a government facility on Plum Island in Long Island Sound. The detectors would be displaced slightly from the center of the neutrino beam, which has the advantage of suppressing unwanted higher energy neutrinos. The four-detector scheme would allow the experiment to be constructed in stages. The first stage, with the furthest detector at 24 km, would be sensitive to ν_μ disappearance at a statistically compelling (3-5 σ) level down to $\Delta m^2 \sim 5 \times 10^{-3} \text{eV}^2$ for $\sin^2 2\theta = 1$, and $\Delta m^2 \sim 10^{-2}$

eV^2 for $\sin^2 2\theta \sim 0.5$, covering the entire range suggested by the atmospheric neutrino anomaly. The second stage, including the detectors at 67 km, would extend the range of Δm^2 to values smaller by a factor of ~ 2 . The statistical significance for $\nu_\mu \rightarrow \nu_e$ appearance would be much larger. The sensitivity of this experiment in both the ν_μ disappearance mode and the $\nu_\mu \rightarrow \nu_e$ appearance channel are shown in Figure 6 and Figure 7, respectively.

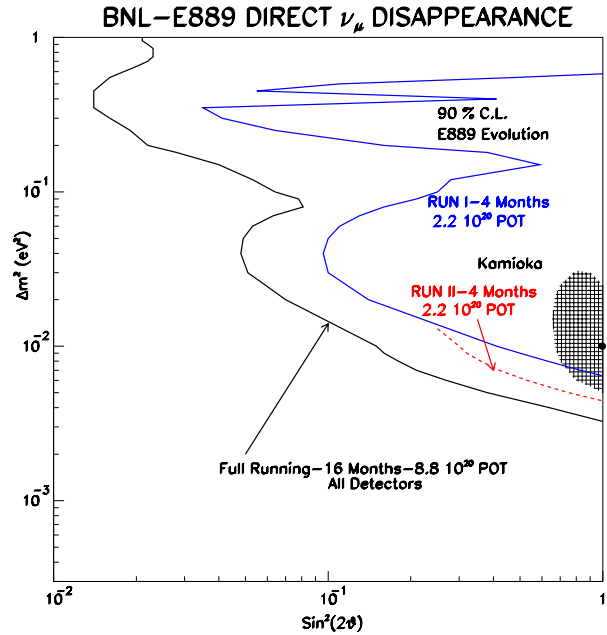


Figure 6: BNL E889 limit curves for ν_μ disappearance.

KEK The KEK proton synchrotron can produce extracted proton beams of 12 GeV at an intensity of 4×10^{12} every 2.5 seconds. A modest upgrade under consideration can provide an intensity of 7.5×10^{12} every 1 second. A proposal is under discussion of using an upgraded PS beam to send neutrinos to the SuperKamiokande detector, located 250 km from the KEK site.

12.2.2 $\nu_\mu \rightarrow \nu_\tau$

FNAL To do both a short and long baseline experiment using the same beamline is an ideal strategy for exploring the question of neutrino mass. The unique feature of such a program at Fermilab is that both the short and long-baseline experiments can be designed to exploit the high-energy feature of the Main Injector - τ appearance. Over the past few years several options for a long-baseline site from the Fermilab beam have been considered, including that of the IMB detector in Cleveland, Ohio, the DUMAND detector in Hawaii, and the Soudan 2 detector in Tower-Soudan, Minnesota. In 1990 members of the Soudan 2 collaboration submitted a pro-

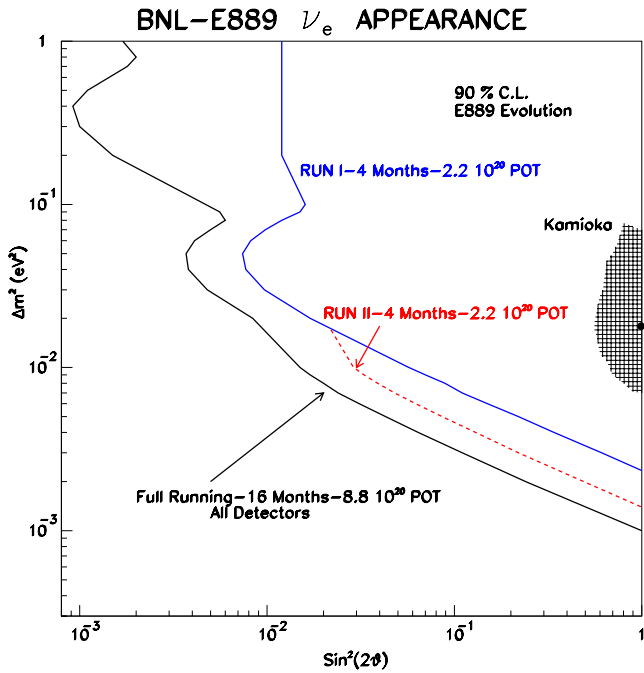


Figure 7: BNL E889 limit curves for $\nu_\mu \rightarrow \nu_e$ oscillations.

posal, P-822, to use the existing Soudan 2 detector to probe the region of parameter space suggested by the atmospheric-neutrino deficit.

A far detector distance between 500 and 1000 km is appropriately matched to the average neutrino energy of 15-20 GeV which can be produced by a horn focussed neutrino beam from the Main Injector 120 GeV protons. The major complication with such a beam is that it must be extracted and brought to a 58 mr downward bend angle, requiring the beamline enclosures and the experimental hall to be significantly below grade, and hence at increased cost due to the civil construction aspect of the project. Because of the financial investment required for such a beam, considerable debate has gone into the question of what the potential reach of an experiment using such a beam should be.

In spring 1994, Fermilab called for Expressions of Interest from the user community for long baseline experiments. Three were received, and though there were technical differences, all three emphasized the advantage that the high-energy Main Injector provides for doing appearance experiments in the channel $\nu_\mu \rightarrow \nu_\tau$. At the June 1994 Fermilab PAC meeting, the PAC strongly endorsed the idea that Fermilab proceed with further development of the Conceptual Design Report for a beamline which will provide for both short and long baseline experiments. Members of the long baseline EOI's were encouraged to join forces and form a strong collaboration to build a detector with the capability of "seeing" τ leptons.

Such a collaboration has been formed and the group has submitted a full proposal, P-875 (a.k.a MINOS) for a 10 kton detector to be located in a new cavern adjacent to the existing Soudan 2 detector [150]. The sensitivity of this experiment to both $\nu_\mu \rightarrow \nu_\tau$ and $\nu_\mu \rightarrow \nu_e$ oscillations are shown in Figure 8 and Figure 9, respectively.

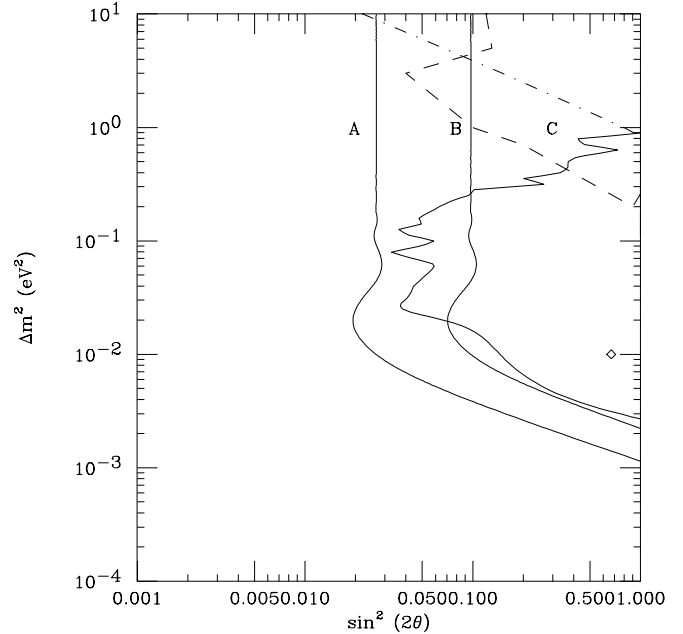


Figure 8: MINOS two year 90% CL limit curves for $\nu_\mu \rightarrow \nu_\tau$ oscillations. Curves A, B and C represent different rate comparisons and energy measurements which can be made in the experiment. The dashed curve shows measured limits from the CDHS experiment, and the dot-dashed curve show FNAL E-531 limits. The diamond is the Kamiokande best-fit point.

CERN At CERN studies have been done to show that it is technically feasible to send a neutrino beam to the Gran Sasso Laboratory in Italy or even to the Superkamiokande detector in Japan, which both happen to be in favorable directions for using existing or planned beamlines. The possibility of pointing a beam toward the NESTOR detector in Greece is also being discussed. The most cost-effective of these options is the beam to Gran Sasso, 732 km from CERN. Such a beamline would share facilities with the planned transfer line from the SPS to the LHC. The detector would be the proposed ICARUS detector [151].

The optimal conditions for $\nu_\mu \rightarrow \nu_e$ oscillations with ICARUS and a CERN SPS beam are obtained with a low proton energy (120 GeV, 3×10^{13} protons on target every 3.6 seconds). For the $\nu_\mu \rightarrow \nu_\tau$ oscillations, a higher beam energy is better suited. If the CERN SPS can deliver 3×10^{13} 450 GeV protons on target every 7.2

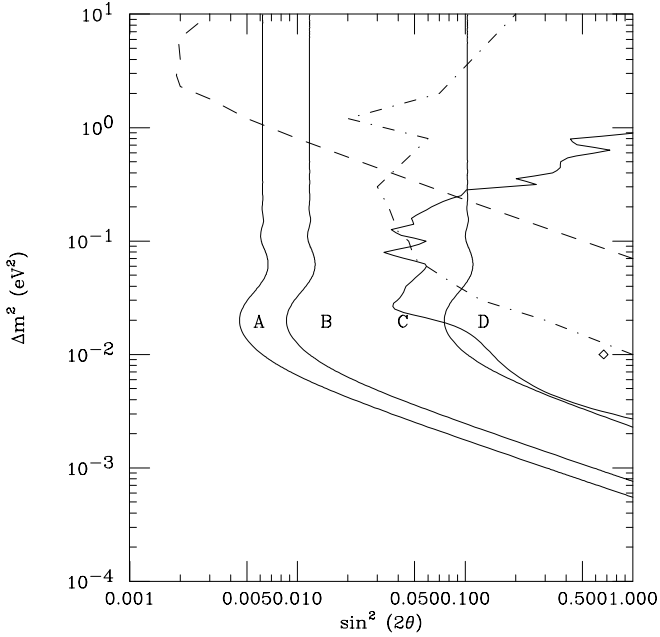


Figure 9: MINOS two year 90% CL limit curves for $\nu_\mu \rightarrow \nu_e$ oscillations. Curves A, B, C and D represent different rate comparisons and energy measurements which can be made in the experiment. The dashed curve shows measured limits from the BNL E-776 experiment, and the dot-dashed curve shows the Bugey 4 reactor experiment limits. The diamond is the Kamiokande best-fit point.

sec, the sensitivity of ICARUS for one year of data taking extends to $\sin^2 2\theta = 5 \times 10^{-2}$ and $\Delta m^2 = 2 \times 10^{-3} \text{ eV}^2$.

Proponents of a long-baseline oscillation program at CERN are proposing that the program could take place naturally in the period between the end of the LEP program and the beginning of the LHC program, *i.e.*, early in the next decade.

12.3 Comparison of Long Baseline Options

A strict comparison of differing options for a neutrino oscillation experiment should be done in the Δm^2 - $\sin^2 2\theta$ plane. Even then, one experiment may have a sensitivity to a lower Δm^2 while the other may reach lower $\sin^2 2\theta$. The preference of one over the other is then strictly a matter of physics value judgement. Nevertheless, some qualitative comparisons of the proposed long baseline experiments are possible. An experiment's sensitivity to mixing angle depends on the test and statistics. The mass sensitivity then also depends on L and the neutrino energy distribution.

This can be made a bit more quantitative. An experiment is generally sensitive to oscillations above some minimum probability of oscillation, or can set a limit at that probability, which we call P_{min} . Then the limit on $\sin^2 2\theta$ at high Δm^2 is at $2 \times P_{min}$. Likewise, the mass

limit at maximal mixing is approximately

$$\Delta m^2 = \frac{\langle E_\nu \rangle \sqrt{P_{min}}}{1.27L}, \quad (35)$$

where Δm^2 , L , and E_ν are respectively in eV^2 , km, and GeV. Since the slope of the limit curve at $\sin^2 2\theta = 1$ is $-1/2$, this almost entirely defines the limit curve, up to the energy distribution and some oscillatory behavior near the first few oscillations at the average E_ν . Then the value of P_{min} depends only on the test, the statistics, and possible systematic limitations. For the most favorable tests, $P_{min} \sim 1.5/\sqrt{N}$ at 90% CL, where N is the number of events measured at the far detector. For tests which involve kinematic cuts or particular decay modes, P_{min} is worse (larger) by the detection efficiencies and branching ratios.

The statistics which an experiment can achieve depends on the neutrino flux, the detector size, the distance, and the neutrino energy distribution. The event rate is proportional to the integrated neutrino flux, which in turn depends on both the duration of the experiment and the fraction of accelerator cycles that can be devoted to a neutrino program.

A higher energy beam gives more neutrino events due to the rising ν cross section. There are also more secondaries produced, and on average they are boosted more in the forward direction. On the other hand, a higher energy beam has more time between spills, less secondary decays in a fixed length beam pipe, and the Δm^2 sensitivity decreasing as $1/\langle E_\nu \rangle$. For tests that require the presence of a τ lepton in the final state, the energy must be significantly above the ν_τ charged current threshold. A 120 GeV proton beam, for example, provides neutrinos with an energy distribution such that $\langle \sigma_\tau / \sigma_\mu \rangle \sim 0.25$, while a 400 GeV beam is required for that ratio to reach 0.50. The lower energy beams at BNL or KEK will not make τ 's by charged current processes.

When realistic detector sizes, running conditions, and accelerator parameters are used, the Fermilab proposal, CERN ICARUS proposal, BNL E899, and KEK to SuperKamiokande proposal all reach similar sensitivities of 5-8% in $\sin^2 2\theta$ and $2 - 3 \times 10^{-3} \text{ eV}^2$ in Δm^2 . The BNL proposal as written has a small disadvantage in Δm^2 sensitivity (limits will only improve as $N^{1/4}$ as opposed to $N^{1/2}$ in $\sin^2 2\theta$), but recent thoughts about placing a far detector at 67 km would overcome that difference. All of these long baseline proposals would cover the region of neutrino oscillation parameter space suggested by the atmospheric neutrino deficit.

A much larger 10-20 kT new detector for the Fermilab to Soudan long baseline experiment, as endorsed by the Fermilab PAC, would increase the sensitivity to lower mixing angle. However, the angles motivated by the atmospheric neutrinos are much larger and in fact are near maximal. Of course, the addition of such a mas-

sive new detector will need to be balanced against cost and available resources.

There are two other important qualitative differences between the low energy experiments (BNL, KEK), for which $\langle E_\nu \rangle \sim 1$ GeV, and higher energy $\langle E_\nu \rangle \sim 15$ GeV (FNAL, CERN) long baseline proposals. The first is that the lower energy experiments are more similar to the energy of the atmospheric neutrino beam. It is possible, for example, that a non-neutrino-oscillation explanation of the atmospheric anomaly could better be tested at a similar energy. The other involves the number of independent tests of $\nu_\mu \leftrightarrow \nu_\tau$ oscillations which can be performed above and below ν_τ charged current threshold. Each test will have its own unique backgrounds and systematic challenges.

13 Summary

We have attempted to review the broad based attack presently being made by both the theoretical and experimental communities on the intriguing and outstanding questions of neutrino mass and mixing. From the outset of this project it was recognized that this would be a topic which unabashedly crosses the traditional interdisciplinary boundaries of high-energy and nuclear physics, cosmology and astrophysics. The conveners of this group as well as the many contributors knew that while boundaries are usually easy to cross, barriers most often are not. We found that, from the standpoint of the physics questions, there were no fundamental boundaries. Barriers imposed by competition for funding and resources are, however, difficult to ignore and extremely difficult to cross.

Neutrino physics, particularly the study of the intrinsic properties of neutrinos, is a subject that has important implications for the disciplines of elementary particle physics, nuclear physics, astrophysics, and cosmology. Forty years after the first direct detection of neutrino interactions with matter, our knowledge of these elusive elementary particles may be summarized as follows. The three neutrino flavors ν_e , ν_μ and ν_τ (and their antiparticles) carry linear and angular momentum (left-handed ν and right-handed $\bar{\nu}$) and an assigned quantum number to specify the lepton family to which they belong. All other fundamental properties, *e.g.*, mass, charge, magnetic dipole moment, and whether they mix with one another, are known only by upper limits. Indeed, it is not known whether the neutrino is a Dirac particle with a distinct antiparticle or a Majorana particle, *i.e.*, its own antiparticle. In the search for physics beyond the Standard Model, new information in the neutrino sector is likely to make an important, perhaps vital, contribution.

For astrophysics, neutrinos probe the interior of stars early and late in their lifetimes. They are the coolant of neutron stars left from supernovae, and provide a poten-

tial thermometer for a precision temperature measurement of our sun's core. Neutrino astrophysics has become a recognized discipline in the last decade.

In the cosmological Big Bang Model, neutrinos decoupled relatively early in the evolution of the universe. This guarantees that they have a substantial relic abundance today if they are stable and do not annihilate. Their intrinsic properties are constrained by cosmological consequences, and, in turn, improved knowledge of neutrino properties would constrain cosmological models of the early universe. If any neutrinos have rest masses in the electron-volt region, they would contribute to the non-baryonic dark matter, and perhaps significantly to the total mass of the universe.

The suggestion was offered in the 1960's that oscillations among neutrino flavors might occur with rates dependent on neutrino mass and mixing amplitude. For the first time, there are reliable data indicating the occurrence of resonant and vacuum neutrino oscillations from studies of solar and atmospheric neutrinos. In an effort to confirm or repudiate these empirical clues, new experiments are being mounted and proposals for new experiments are being made. Because the potential importance of the envisioned results is well recognized, the proposals must be treated seriously even at a time of restricted funding. The relevant ranges of Δm^2 and $\sin^2 2\theta$ are now well defined, and the planned and proposed experiments should be able to establish or exclude them definitively.

For the first time, direct measurements placing limits on the mass of the electron-neutrino in the region of electron-volts have been made in the past few years. A common feature of all of these experimental results is an anomalous excess of counts near the endpoint. This anomaly is indicative of a misconception—perhaps a serious one—on our part, and experiments to probe its nature and pursue the hint it offers are crying to be done.

Also for the first time, compelling direct measurements of the rates for double beta decay involving two neutrinos have been made recently. These measurements set the stage for incisive attempts to observe double beta decay in the absence of neutrinos and possibly discover the Majorana identity of the neutrino. This is an area of neutrino physics that is not costly but is of fundamental importance.

The field of neutrino physics is diverse and carried out non-centrally in self-contained experiments in university laboratories, deep underground sites, and accelerators. In part for this reason, it appears to involve a small community with few needs. But in truth, it is a world-wide effort pursued by many physicists, which often requires well-instrumented, massive apparatus. Experiments, whether large or small, require adequate long term support. Given the great scientific potential of physics involving neutrino mass and lepton flavor mix-

ing, the enterprise deserves support beyond the level at which it now functions.

References

- [1] *Review of Particle Properties*, L. Montanet *et al.*, *Phys. Rev. D* **50**, 1173 (1994).
- [2] G. F. Smoot *et al.*, *Astrophys. J.* **396**, L1 (1992); A. de Oliveira Costa and G. F. Smoot, astro-ph/9412003.
- [3] A. Klypin *et al.*, *Astrophys. J.* **416**, 1 (1993); M. Davis, F. Summers, and D. Schlegel, *Nature* **359**, 393 (1992); D. Schlegel *et al.*, *Astrophys. J.* **427**, 512 (1994); Y. P. Jing *et al.*, *Astron. Astroph.* **284**, 703 (1994); R. Nolthenius, A. Klypin, and J. Primack, *Astrophys. J. Lett.* **422**, L45 (1994); J. Primack *et al.*, SCIPP 94/28.
- [4] For detailed reviews, see G. Gelmini and E. Roulet, UCLA/94/TEP/36; P. Langacker in *Testing The Standard Model*, ed. M. Cvetič and P. Langacker (World, Singapore, 1991) p. 863, and in *Beyond the Standard Model III*, ed S. Godfrey and P. Kalyniak (World, Singapore, 1993) p. 91; B. Kayser, F. Gibrat-Debu, and F. Perrier, *The Physics of Massive Neutrinos*, (World Scientific, Singapore, 1989).
- [5] Y. Zeldovich, DAN SSSR **86**, 505 (1952); E. S. Konopinski and M. Mahmoud, *Phys. Rev.* **92**, 1045 (1953).
- [6] G. B. Gelmini and M. Roncadelli, *Phys. Lett. B* **99**, 411 (1981); H. Georgi *et al.*, *Nucl. Phys. B* **193**, 297 (1983).
- [7] D. Schaile, plenary talk presented at the *27th International Conference on High Energy Physics*, Glasgow, July 1994.
- [8] M. Gell-Mann, P. Ramond, and R. Slansky, in *Supergravity*, ed. F. van Nieuwenhuizen and D. Freedman, (North Holland, Amsterdam, 1979) p. 315; T. Yanagida, *Proc. of the Workshop on Unified Theory and the Baryon Number of the universe*, KEK, Japan, 1979; S. Weinberg, *Phys. Rev. Lett.* **43**, 1566 (1979).
- [9] R. N. Mohapatra and G. Senjanovic, *Phys. Rev. D* **23**, 165 (1981).
- [10] See S. A. Bludman, D. C. Kennedy, and P. Langacker, *Nucl. Phys. B* **374**, 373 (1992) and *Phys. Rev. D* **45**, 1810 (1992), and references therein.
- [11] A. Zee, *Phys. Lett. B* **93**, 389 (1980); **161**, 141 (1985); *Nucl. Phys. B* **264**, 99 (1986). For later references, see [4].
- [12] For a review of limits on neutrino magnetic moments, see [1].
- [13] S. Bertolini and A. Santamaria, *Nucl. Phys. B* **310**, 714 (1988); **315**, 558 (1988).
- [14] T. P. Walker *et al.*, *Astrophys. J.* **376**, 51 (1991).
- [15] P. Langacker, UPR-0401T; R. Barbieri and A. Dolgov, *Phys. Lett. B* **237**, 440 (1990); *Nucl. Phys. B* **349**, 743 (1991); K. Kainulainen, *Phys. Lett. B* **244**, 191 (1990); K. Enqvist, K. Kainulainen, and J. Maalampi, *Phys. Lett. B* **244**, 186 (1990); **249**, 531 (1990); M. J. Thomson and B. H. J. McKellar, *Phys. Lett. B* **259**, 113 (1991); X. Shi, D. Schramm, and B. Fields, *Phys. Rev. D* **48**, 2563 (1993).
- [16] N. Hata, private communication. For updated figures, see "<http://dept.physics.upenn.edu/~www/neutrino/solar.html>".
- [17] For recent reviews and discussions, see S. Bludman, *Phys. Rev. D* **45**, 4720 (1992); G. Gelmini, *Neutrino Physics*, H. V. Klapdor and P. Povh, eds. (Springer-Verlag, Berlin, 1988) p. 44; E. W. Kolb and M. Turner, *The Early universe* (Addison-Wesley, Redwood City, 1989).
- [18] G. Steigman and M. S. Turner, *Nucl. Phys. B* **253**, 375 (1985).
- [19] K. Hirata *et al.*, *Phys. Rev. Lett.* **58**, 1490 (1987).
- [20] R. M. Bonita *et al.*, *Phys. Rev. Lett.* **58**, 1494 (1987).
- [21] W. D. Arnett *et al.*, *Ann. Rev. Astron. Astrophys.* **7**, 629 (1989); A. Burrows, *Ann. Rev. Nucl. Part. Sci.* **40**, 181 (1990).
- [22] T. J. Loredo and D. Q. Lamb, *Proceedings of Relativistic Astrophysics*, Dallas, 1988, p. 601.
- [23] A. Burrows, D. Klein, and R. Gandhi, *Phys. Rev. D* **45**, 3361 (1992).
- [24] G. T. Ewan *et al.*, in *Proceedings of the Supernova Watch Workshop*, Santa Monica, California, (1990).
- [25] R. G. H. Robertson *et al.*, in *Perspectives in Neutrinos, Atomic Physics, and Gravitation*, XIII'th Moriond Workshop, Villars-sur-Ollon, Switzerland, (1993).

- [26] E. S. Hafen *et al.*, in *Proceedings of the Supernova Watch Workshop*.
- [27] D. B. Cline *et al.*, in the International Conference on Neutrino Astrophysics, Takayama, Kamioka, Japan (1992).
- [28] L. M. Krauss, P. Romanelli, D. Schramm, R. Lehrer, *Nucl. Phys. B* **380**, 507 (1992).
- [29] D. B. Cline *et al.*, *Phys. Rev. D* **50**, 720 (1994).
- [30] C. Pennypacker *et al.*, in *Preliminary Estimates of Core-Collapse Supernova Rates from the Berkeley Automated Supernova Search*, Lawrence Berkeley Laboratory Preprint, LBL-3059 (1991); *Ap. Astro. J* **384**, L9 (1992).
- [31] M. M. Lowry, private communication.
- [32] V. M. Lobashev *et al.*, Proc. 16th Int. Conf. Neutrino Physics and Astrophysics, *Neutrino '94*, Eilat, Israel, May 29 - June 3, 1994, to be published.
- [33] V. A. Lyubimov, Proc. 13th Int. Conf. Neutrino Physics and Astrophysics, *Neutrino '88*, ed. J. Schneps *et al.* (World Scientific, Singapore, 1989) p. 2.
- [34] R. G. H. Robertson *et al.*, *Phys. Rev. Lett.* **67**, 957 (1991).
- [35] E. Holzschuh, M. Fritschi, and W. Kündig, *Phys. Lett. B* **287**, 381 (1992).
- [36] H. Kawakami *et al.*, *Phys. Lett. B* **256**, 105 (1991).
- [37] Ch. Weinheimer *et al.*, *Phys. Lett. B* **300**, 210 (1993).
- [38] D. Decman and W. Stoeffl, submitted to *Phys. Rev. Lett.* (1994).
- [39] G. J. Clark and M.A. Frisch, Proc. Santa Fe Meeting of Div. of Particles and Fields of the APS, ed. T. Goldman and M. M. Nieto (World Scientific, Singapore 1984), p. 245.
- [40] M. Fink and H. Wellenstein, unpublished.
- [41] B. Jeckelmann *et al.*, *Phys. Rev. Lett.* **56**, 1444 (1986).
- [42] R. Abela *et al.*, *Phys. Lett. B* **146**, 431 (1984).
- [43] K. Hikasa *et al.*, *Phys. Rev. D* **45**, S1 (1992).
- [44] M. Daum *et al.*, *Phys. Lett. B* **265**, 425 (1991).
- [45] R. Frosch, private communication (1992).
- [46] B. Jeckelmann, P. F. A. Goudsmit, and H. J. Leisi, *Phys. Lett. B* **335**, 326 (1994).
- [47] H. B. Anderhub *et al.*, *Phys. Lett. B* **114**, 76 (1982).
mohapatra
- [48] G. B. Mills *et al.*, *Phys. Rev. Lett.* **54**, 624 (1985).
- [49] P. Burchat *et al.*, *Phys. Rev. Lett.* **54**, 2489 (1985).
- [50] C. Matteuzzi *et al.*, *Phys. Rev. D* **32**, 800 (1985).
- [51] H. Albrecht *et al.*, *Phys. Lett. B* **163**, 404 (1985).
- [52] S. Abachi *et al.*, *Phys. Rev. Lett.* **56**, 1039 (1986).
- [53] S. Csorna *et al.*, *Phys. Rev. D* **35**, 2747 (1987).
- [54] H. Albrecht *et al.*, *Phys. Lett. B* **202**, 149 (1988).
- [55] R. Balest *et al.*, *Phys. Rev. D* **47**, 3671 (1993).
- [56] D. Cinabro *et al.*, *Phys. Rev. Lett.* **70**, 3700 (1993).
- [57] *Sensitivity of Future High-Luity e^+e^- Colliders to a Massive τ Neutrino*, J. J. Gomez-Cadenas, CERN-PPE/94-12, Jan. 1994.
- [58] T. Bernatowicz *et al.*, *Phys. Rev. Lett.* **69**, 2341 (1992).
- [59] A. Balysh *et al.*, *Phys. Lett. B* **283**, 32 (1992).
- [60] S. R. Elliott *et al.*, *Phys. Rev. Lett.* **56**, 2582 (1986).
- [61] V. Gribov and B. Pontecorvo, *Phys. Lett. B* **28**, 493 (1969); S. M. Bilenky and B. Pontecorvo, *Phys. Rep.* **41**, 225 (1978).
- [62] L. Wolfenstein, *Phys. Rev. D* **17**, 2369 (1978); *Phys. Rev. D* **20**, 2634 (1979).
- [63] S. P. Mikheyev and A. Yu. Smirnov, *Sov. J. Nucl. Phys.* **42**, 913 (1986); *Nuovo Cimento C* **9**, 17 (1986).
- [64] W.-K. Kwong and S. P. Rosen, *Phys. Rev. Lett.* **73**, 369 (1994).
- [65] N. Hata, S. Bludman, and P. Langacker, *Phys. Rev. D* **49**, 3622 (1994).
- [66] N. Hata and P. Langacker, UPR-0625T.
- [67] J. N. Bahcall, IASSNS-AST 94/37.
- [68] V. Castellani *et al.*, ASTROPH-9405018, *Phys. Rev. D* **50**, 4749 (1994).

- [69] S. Degl'Innocenti, G. Fiorentini, and M. Lissia, INFNFE-10-94.
- [70] X. Shi, D. Schramm, and S. P. Dearborn, *Phys. Rev. D* **50**, 2414 (1994).
- [71] J. N. Bahcall and M. H. Pinsonneault, *Rev. Mod. Phys.* **64**, 885 (1992) and references therein; S. Turck-Chièze and I. Lopes, *Astrophys. J.* **408**, 347 (1993).
- [72] R. Davis Jr., *Frontiers of Neutrino Astrophysics*, ed. by Y. Suzuki and K. Nakamura (Universal Academy Press, Inc., Tokyo, Japan, 1993), p. 47.
- [73] K. Lande, invited talk, *Solar Neutrinos and Neutrino Astrophysics*, Institute for Nuclear Theory, University of Washington, Feb. 22 - May 31, 1994 (unpublished).
- [74] A. Garcia, E. G. Adelberger, P. V. Magnus, H. E. Swanson, O. Tengblad, and the Isolde Collaboration, *Phys. Rev. Lett.* **67**, 3654 (1991).
- [75] K. S. Hirata, *et al.*, *Phys. Rev. Lett.* **63**, 16 (1989).
- [76] K. S. Hirata, *et al.*, *Phys. Rev. D* **44**, 2241 (1991).
- [77] A. Suzuki, KEK Preprint 93-96, 1993.
- [78] J. N. Bahcall, *Neutrino Astrophysics* (Cambridge University Press, Cambridge, England, 1989).
- [79] V. A. Kuz'min, *Sov. Phys. - JETP* **22**, 1059 (1966).
- [80] J. N. Bahcall, B. T. Cleveland, R. Davis, Jr., *et al.*, *Phys. Rev. Lett.* **40**, 1351 (1978).
- [81] A. I. Abazov *et al.*, *Phys. Rev. Lett.* **67**, 3332 (1991).
- [82] J. N. Abdurashitov *et al.*, *Phys. Lett. B* **328**, 234 (1994).
- [83] P. Anselmann *et al.*, *Phys. Lett. B* **285**, 376 (1992).
- [84] P. Anselmann, *Phys. Lett. B* **314**, 445 (1993).
- [85] J. S. Nico, Proc. Int. Conf. on High-Energy Physics, *ICHEP 1994*, Glasgow, July 18-29, 1994 (to be published).
- [86] P. Anselmann *et al.*, *Phys. Lett. B* **327**, 377 (1994).
- [87] P. Anselmann *et al.*, Gallex preprint GX65-1994.
- [88] N. Hata and P. Langacker, *Phys. Rev. D* **50**, 632 (1994); S. Bludman *et al.*, *Phys. Rev. D* **47**, 2220 (1993).
- [89] X. Shi, D. Schramm, and J. Bahcall, *Phys. Rev. Lett.* **69**, 717 (1992); X. Shi and D. Schramm, *Phys. Lett. B* **283**, 205 (1992).
- [90] J. M. Gelb, W.-K. Kwong and S. P. Rosen, *Phys. Rev. Lett.* **69**, 1864 (1992).
- [91] P. I. Krastev and S. T. Petcov, *Phys. Lett. B* **299**, 99 (1993).
- [92] G. L. Fogli, E. Lisi, and D. Montanino, *Phys. Rev. D* **49**, 3626 (1994).
- [93] G. Fiorentini *et al.*, *Phys. Rev. D* **49**, 6298 (1994).
- [94] P. I. Krastev and S. T. Petcov, *Phys. Rev. Lett.* **72**, 1960 (1994) and SISSA-41-94-EP, and references therein.
- [95] N. Hata, UPR-0605T.
- [96] A. Acker and S. Pakvasa, *Phys. Lett. B* **320**, 320 (1994).
- [97] M. B. Voloshin, M. I. Vysotskii, and L. B. Okun, *Yad. Fiz.* **44**, 677 (1986) [*Sov. J. Nucl. Phys.* **44**, 440 (1986)].
- [98] E. K. Akhmedov, FTUV-94-26; E. K. Akhmedov, A. Lanza, and S. T. Petcov, *Phys. Lett. B* **303**, 85 (1994), and references therein.
- [99] H. H. Chen *et al.*, *Phys. Rev. Lett.* **55**, 1534 (1985); G. Aardsma *et al.*, *Phys. Lett. B* **194**, 321 (1987); G. T. Ewan *et al.*, Sudbury Neutrino Observatory Proposal SNO-87-12 (1987).
- [100] A. J. Baltz and J. Weneser, BNL-60387, *Phys. Rev. D* **35**, 528 (1987).
- [101] E. D. Carlson, *Phys. Rev. D* **34**, 1454 (1986).
- [102] N. Hata and P. Langacker, *Phys. Rev. D* **48**, 2937 (1993), and references therein.
- [103] J. Engel, S. Pittel, and P. Vogel, *Phys. Rev. C* **50**, 1702 (1994).
- [104] G. Ranucci for the Borexino Collaboration, *Nucl. Phys. (Proc. Suppl.)* **32**, 149 (1993); C. Arpasella *et al.*, in *Borexino at Gran Sasso: Proposal for a real-time detector for low energy solar neutrinos*, Volumes I and II, University of Milan, INFN report (unpublished).
- [105] P. Cennini *et al.*, *Nucl. Instrum. Meth. A* **345**, 230 (1994).

- [106] Heron Collaboration, *Phys. Rev. Lett.* **58**, 2498 (1987); *Phys. Rev. Lett.* **68**, 2429 (1992); *Rev. Sci. Instrum.* **63**, 230 (1992); *J. Low Temp. Phys.* **93**, 709 (1993); *ibid* **93**, 785 (1993); *ibid* **93**, 715 (1993).
- [107] J. Seguinot, T. Ypsilantis, and A. Zichini, *A High Rate Solar Neutrino Detector with Energy Determination*, LPC92-31, College de France, 12/8/92.
- [108] M. Goodman (Soudan 2), *Nucl. Phys.* (Proc. Suppl.) **38**, 337 (1995).
- [109] M. Aglietta *et al.*, (NUSEX), *Europhysics Letters* **8**, 611 (1989).
- [110] R. Becker-Szendy *et al.*, *Phys. Rev. D* **49**, 3720 (1992); and D. Casper, Ph. D. thesis, University of Michigan, 1990.
- [111] Kamiokande presentation at Neutrino 1994 (Eilat).
- [112] M. Circella *et al.*, *Proc. 23rd Int. Cosmic Ray Conf.* (Calgary) **4**, 503 (1993).
- [113] D. Müller *et al.*, (HEAT Collaboration), *Proc. 22nd Int. Cosmic Ray Conf.* (Dublin), **2**, 177 (1991).
- [114] D. H. Perkins, *Astroparticle Physics* **2**, 249 (1994).
- [115] Y. Fukuda *et al.*, (Kamiokande collaboration), *Phys. Lett. B* **335**, 237 (1994).
- [116] K. S. Hirata *et al.*, (Kamiokande Collaboration), *Phys. Lett. B* **280**, 146 (1992). This paper reported on a 4.92 kT yr exposure. The exposure for sub-GeV, fully contained events is now 7.7 kT yr [115].
- [117] H. Meyer, for the Fréjus collaboration, talk presented at Snowmass, July 7, 1994.
- [118] R. Becker-Szendy *et al.*, (IMB Collaboration), *Phys. Rev. D* **46**, 3720 (1992).
- [119] Ch. Berger *et al.*, (Fréjus), *Phys. Lett. B* **245**, 305 (1990), **227**, 489 (1989).
- [120] M. Honda, K. Kasahara, K. Hidaka, and S. Midorikawa, *Phys. Lett. B* **248**, 193 (1990).
- [121] R. Becker-Szendy *et al.*, *Phys. Rev. Lett.* **69**, 1010 (1992).
- [122] M. Goodman, *Proceedings of the Atmospheric Neutrino Workshop*, 6-8 May 1993, LSU-HEPA-93-6.
- [123] T. Kajita, *Proceedings of the Atmospheric Neutrino Workshop*, 6-8 May 1993, LSU-HEPA-93-6.
- [124] D. Michael, private communication.
- [125] L. V. Volkova, *Sov. J. Nucl. Phys.* **31**, 1510 (1980).
- [126] E. Eichten, I. Hinchcliffe, K. Lane, and C. Quigg, *Rev. Mod. Phys.* **56**, 579 (1984) [**56**, 1065E (1986)].
- [127] W. Frati, T. K. Gaisser, A. K. Mann, and T. Stanev, *Phys. Rev. D* **48**, 1140 (1993).
- [128] M. Mori *et al.*, *Phys. Lett. B* **270**, 89 (1991).
- [129] A. V. Butkevich, L. G. Dedenko, and I. M. Zheleznykh, *Sov. J. Nucl. Phys.* **50**, 90 (1989).
- [130] V. Agrawal, T. K. Gaisser, P. Lipari, and T. Stanev (unpublished).
- [131] J. F. Owens, *Phys. Lett. B* **266**, 126 (1991).
- [132] D. Michael for the MACRO Collaboration, talk presented at Snowmass, July 7, 1994.
- [133] M. M. Boliev *et al.*, (Baksan Collaboration), in *Proc. 3rd Int. Workshop on Neutrino Telescopes*, Venice, 1991 (ed. M. Baldo-Ceolin) p. 235.
- [134] G. Barr, T. K. Gaisser, and T. Stanev, *Phys. Rev. D* **39**, 3532 (1989).
- [135] E. V. Bugaev and V. A. Naumov, *Phys. Lett. B* **232**, 391 (1989).
- [136] J. Engel, E. Kolbe, K. Langanke, and P. Vogel, *Phys. Rev. D* **48**, 3048 (1993).
- [137] G. L. Fogli, E. Lisi, and D. Montanino, *Phys. Rev. D* (to be published).
- [138] The San Onofre Collaboration, *Proposal for the San Onofre Neutrino Oscillation Experiment*, Caltech, January 1994, unpublished.
- [139] The Chooz Collaboration, *Proposal to Search for Neutrino Vacuum Oscillations to $\Delta m^2 = 10^{-3} \text{ eV}^2$ Using a 1 Km Baseline Reactor Neutrino Experiment*, Drexel University, June 1993, unpublished.
- [140] The Chooz Collaboration, *Chooz Neutrino Experiment Home Page*, http://duphy4.physics.drexel.edu/chooz_pub/.
- [141] F. Boehm *et al.*, *A Large, Low-Energy Neutrino Detector for Neutrino Oscillations and Supernovae Watch*, *Nucl. Instrum. Meth. A* **300** 395 (1991).

- [142] R. Steinberg *et al.*, *PERRY: A Reactor Neutrino Oscillation Experiment Sensitive to $\Delta m^2 = 10^{-4} \text{ eV}^2$* , in *The FERMLAB Meeting DPF92*, ed. C.H. Albright, (World Scientific, Singapore, 1993), p. 1296.
- [143] D.H. White, Invited Paper, Long-Range Planning Town Meeting on Electroweak Interactions, Astrophysics, and Non-Accelerator Experiments, Berkeley, CA, Feb. 4-5, 1995 (unpublished).
- [144] KARMEN Collaboration, B. Armbruster *et al.*, *Nucl. Phys. (Proc. Suppl.)* **38**, 235 (1995).
- [145] CHORUS Collaboration, N. Armenise *et al.*, CERN-SPSC/90-42 (1990).
- [146] NOMAD Collaboration, P. Astier *et al.*, CERN-SPLC/91-21 (1991).
- [147] N. Ushida *et al.*, *Phys. Rev. Lett.* **57**, 2897 (1986).
- [148] E-803, Muon Neutrino to Tau Neutrino Oscillations (October 1990); Update (october 1993), N. W. Reay, spokesperson.
- [149] *Proposal for a Long Baseline Neutrino Oscillation Experiment at the AGS*, 1993, A. Mann, spokesperson.
- [150] P-875: A Long-baseline Neutrino Oscillation Experiment at Fermilab, February 1995, S. Wojcicki, spokesperson.
- [151] Icarus II Proposal, *A Second-generation Proton Decay Experiment and Neutrino Observatory at the Gran Sasso Laboratory*, LNGS-94/99-II, May 1994.